

**A PHASE-DOMAIN INDUCTION MOTOR MODEL
FOR TRANSIENT STUDIES**

By

THORNLEY O. A. O. MYERS

M.Sc. Elect. Eng., The José Antonio Echeverría
Higher Polytechnic Institute, (Cuba)

A THESIS SUBMITTED IN PARTIAL FULFILLMENT OF
THE REQUIREMENT FOR THE DEGREE OF
MASTER OF APPLIED SCIENCE

in

THE FACULTY OF GRADUATE STUDIES
DEPARTMENT OF ELECTRICAL ENGINEERING

We accept this thesis as conforming to the required standard

THE UNIVERSITY OF BRITISH COLUMBIA

April 1995

© THORNLEY MYERS, 1995

In presenting this thesis in partial fulfilment of the requirements for an advanced degree at the University of British Columbia, I agree that the Library shall make it freely available for reference and study. I further agree that permission for extensive copying of this thesis for scholarly purposes may be granted by the head of my department or by his or her representatives. It is understood that copying or publication of this thesis for financial gain shall not be allowed without my written permission.

Department of Electrical Engineering

The University of British Columbia
Vancouver, Canada

Date 25/04/95

Abstract

The research programme presented in this thesis terminates the first phase in the development of a new and accurate model for transient analysis of induction motors in the phase domain. Modelling the induction machine variables in the phase domain required a new model which when tested in similar conditions with existing models would give comparable results in both transient and steady-state studies. This new model has been developed, and essentially it differs from traditional models in that it works directly with the machine variables such as currents and voltages directly in the phase domain instead of the dq0 coordinates. This required the solution of a series of first order differential equations with time-varying coefficients. The solution method is based on the discretization of the differential equations with the use of the trapezoidal rule of integration. The new model has been used to develop a computer program for transient and steady-state analysis of induction motors.

The new phase domain transient model (PDTM) requires a number of circuit parameters of the induction motor that are not normally supplied by the manufacturer. Consequently, modifications were performed on a computer program that calculates the parameters of the standard 60-Hz equivalent circuit from starting and steady-state characteristics of the motor to obtain the circuit parameters of the PDTM.

The results from the PDTM compare favourably tested with those obtained from the electromagnetic transient program (EMTP) which uses conventional dq0 coordinates to model the induction motor.

TABLE OF CONTENTS

Abstract	ii
Table of Contents	iii
List of Figures	v
Acknowledgement	viii
Dedication	ix
Chapter 1 Introduction	1
1.1 Background and Overview	1
1.2 Motivation for this Thesis	3
1.3 Research Objectives	5
Chapter 2 The Induction Machine	6
2.1 Physical Characteristics.....	6
2.2 Electromagnetic Features of the Induction Machine.....	7
2.3 Induction Machine Circuits.....	9
Chapter 3 The Phase-Domain Model of the Squirrel-cage Induction Machine	16
3.1 Solution technique.....	16
3.2 The Stator Circuit.....	18
3.3 The Rotor Circuits.....	21
3.4 The Combined Stator-Rotor Circuit Analysis.....	26
3.5 Machine Circuit Model Formulation.....	35

Chapter 4 Electromechanical Model and Data	
Requirements for the PDTM	40
4.1 Torque Production in the Induction Machine.....	40
4.2 Predicting Rotor Velocity and Angular Position.....	43
4.3 Data for the PDTM Program.....	44
Chapter 5 Transient Simulations with the PDTM	46
5.1 Simulation Case Study.....	46
Chapter 6 Conclusions	59
Bibliography	61

List of Figures

1. Squirrel-cage rotor-bar cross sections, (a) single cage, (b) deep-bar and (c) double-cage (NEMA).....	7
2. Magnetic characteristics of a loaded two-pole induction motor.....	9
3. A two-pole wye-connected induction machine.....	11
4. Steinmetz single phase equivalent circuit of a three phase induction motor.....	14
5. Equivalent circuit single phase circuit of a three phase deep-bar rotor and double-cage induction motor.....	15
6. Voltage in an inductor in (a) continuous and (b) discrete time domains	17
7. Voltage across a series resistor-inductor branch in continuous and discrete time domains.....	18
8. Stator circuit with series elements and mutual coupling between the phases.....	19
9. Discrete-time equivalent circuit of the stator windings.....	21
10. Deep-bar rotor effects. (a) Leakage flux paths. (b) Circuit representation showing varying inductance.....	22
11. Rotor equivalent circuit. (a) Two rotor circuits in parallel. (b) Rotor circuit one (not short-circuited).....	23
12. Discretized equivalent circuit of the rotor windings.....	25
13. The phases/windings of (a) the stator circuit, (b) rotor circuit one and (c) rotor circuit two.....	26

14. Positive sequence circuit of one phase of the stator and rotor circuits of the induction motor.....	27
15. Negative (a) and zero (b) sequence circuits of stator and rotor circuits in the induction motor.....	29
16. Conversion from 0-1-2 components (zero, positive and negative sequence) to a-b-c components (actual windings).....	30
17. Magnetic interaction of the stator and rotor circuits of the induction motor.....	31
18. Discrete-time model of the induction motor in phase coordinates.....	37
19. No-load stator current (phase a) during startup.....	48
20. Torque characteristics during no-load startup.....	48
21. Rotor speed during no-load startup.....	49
22. Startup stator current (phase a) with a transient mechanical load.....	49
23. Outer rotor startup current (phase a) with a transient mechanical load.....	50
24. Inner rotor startup current (phase a) with a transient mechanical load.....	50
25. Total startup rotor current (phase a) with a transient mechanical load.....	51
26. Motor torque characteristics during startup with a transient mechanical load.....	51
27. Rotor speed during startup with a transient mechanical load.....	52
28. Stator current (phase a) during startup with a constant mechanical load.....	52
29. Torque characteristics during startup with a constant mechanical load.....	53
30. Rotor speed during startup with a constant mechanical load.....	53

31. EMTP simulated stator current (phase a).....	54
32. Stator current (phase a) simulated with the phase-domain transient model.....	55
33. Motor torque characteristics simulated with the EMTP.....	56
34. Motor torque characteristics simulated with the phase-domain transient model....	56
35. Rotor speed simulated with the EMTP.....	57
36. Rotor speed simulated with the phase-domain transient model.....	57

Acknowledgement

There are many persons and organisations that have contributed to the completion of this thesis. Firstly, I would like to thank the Canadian Commonwealth Scholarship and Fellowship Plan (CCSFP) for granting me the opportunity to study here in Canada. Also, I would like to acknowledge the support my employer, the St. Vincent Electricity Services Company Limited (VINLEC). I extend many thanks to Dr. J. R. Martí for his support and guidance throughout the duration of this research project, also, to committee members Dr. Wvong and Dr. Dunford for their careful examination of this thesis. I would also like to acknowledge the support and encouragement of my colleagues in the reaseach power group during difficult and trying times. Finally, I would like to recognise the contribution of my mother Gerladine, Nick, Elaine, and my fiancé Deirdre.

Dedication

I would like to dedicate this thesis to the memory of my grandparents Mr. and Mrs. Edmund Myers who were a constant source of inspiration throughout my young and formative years, also, to the many progressive revolutionaries who despite politically challenging times, continue to fight for a just and equitable socio-economic life for the most disadvantaged and overexploited peoples of the world.

Chapter 1

Introduction

1.1 Background and Overview

The discovery of the law of electromagnetic induction in 1831 by Michael Faraday, followed by the recognition of the rotating magnetic field principle by the Italian physicist G. Ferraris in 1885 set the stage for the rapid industrial and technological advancement in the twentieth century. Their discoveries facilitated the construction of the first commercial type induction machine in 1889 by the Russian Dolivo-Dobrovolsky, with the result that in just over one hundred years electrical machines have become the major consumer of energy in the power systems. It is estimated that between 60 to 70 per cent of the total energy supplied by power systems is consumed by induction machines [3]. Induction machines range from a few watts found in single phase hand powered tools to three phase machines with output of thousands of kilowatts that can be found in pumps and other large industrial drives.

With the above in mind it may now be possible to understand why it is extremely important that power system engineers study the effects of induction machines on power system stability and particularly their effects on transient stability. However, in order to undertake such studies it is important that the engineer has a model which accurately represents the behaviour of the machine within the range of its operating capabilities. With this model, the engineer can be in a position to answer questions such as; the starting time of his machine under any given condition, the starting torque and the maximum torque that the machine can develop in a given situation, and the voltage levels in different

areas of his local system due to the starting of one or more of his machines. Therefore, the model developed for the induction machines must be able to accurately reflect transient conditions as well as steady state operation. The model must also be reliable, accurate, and at the same time present the user with the information for decision making.

The new model developed represents all the machine voltages and currents as phase quantities. There is no need for the utilisation of any reference frame to transform the variables from phase quantities to dq0 coordinates. The time varying mutual inductances between stator and rotor circuits in the differential equation of the voltages are discretized to form equivalent resistances and history voltage sources in each simulated time step. The solution of the discretized inductances in the time-domain for both the stator and rotor circuit voltages gives rise to a large system of equations. The application of linear and matrix algebra theory reduces the system from a 9x9 matrix representation to a 3x3 system. This system of equations is then solved to determine the motor stator and rotor currents, which are subsequently used to determine electromagnetic torque and rotor velocity. The application of this model is done through the development of the PDTM computer program. The program has been written in the ADA-95 programming language.

The model has been developed in conjunction with another program that is used to obtain all the essential electric circuit parameters that are not normally part of the manufacturers data, but are necessary to use the PDTM program for transient studies. This program uses standard machine starting and rated load performance data supplied by the motor manufacturer to obtain stator and rotor resistances and inductances.

Throughout this thesis the reader is provided with a methodological description and clear explanation of the principles on which the squirrel cage induction motor functions, the stages in the development and implementation of the new model, and finally the opportunity to compare the results from the new model with another transient program that uses traditional modelling techniques. Chapter two will describe the theory behind the

induction machine as well as its electrical and magnetic circuitry and essential characteristics which contribute to its widespread application. Towards the end of this chapter there is a discussion on the traditional method of modelling induction machines and how they differ from the current phase domain model.

Chapter three forms the core of this thesis, and it begins by looking at the machine as an electrical device consisting of separate and completely independent electrical circuits. Subsequently, the "three" electrical circuits of the machine are considered as a complete interconnected and interdependent unit. This sets the stage for the circuit development and finally the mathematical formulation of the new model.

The fourth chapter begins by linking the electrical and mechanical equations of the machine. This is followed by a brief description of the procedure used to calculate the motor circuit parameters necessary to perform simulations with the PDTM. The method is based on the traditional equivalent circuit model of the induction machine.

The fifth chapter of the thesis present test cases simulated with the new PDTM and compares the results with those obtained using the EMTP.

The final chapter looks at the conclusion and recommendations that have resulted from the application of phase domain theory to transient analysis studies of the squirrel cage induction machine.

1.2 Motivation for the Thesis

In the field of electrical engineering, as in many other areas of engineering, many numerical and graphical transformations have been developed and used extensively for decades in an effort to overcome perceive mathematical difficulties in solving technical problems. In the realm of machine analysis, investigators have for decades used different

reference frames to change the variables in phase coordinates to variables in a specified reference frame. In induction machine analysis, the mutual inductance between stator and rotor are a function of the rotor position and this gives rise to time-varying coefficients in the voltage equations. The change of variables in this case has been utilised to avoid the complexity that arises as a result of these time varying coefficients in the differential equations.

However, within the past decade the rapid progress in the field of digital computer processing has opened new areas of scientific research and analytical methods. Despite these advances, the modelling of induction motors has continued in much the same manner as it did in the early 1960's with the use of analog computers. At the same time, the size and output of motors have increased substantially as well as their importance and effect on the power system. Thus, there seems to exist the need for more efficient and accurate techniques to model the induction motor.

Within the past ten years electrical utilities have expanded their roles from just suppliers of electrical power to one where they are now concentrating more and more on the loads that they are called upon to supply. Electric motors form a substantial part of this load. At the same time online programs are being developed to assess the effect of these loads on the power system stability during transient and steady-state periods. It is envisioned that a program for transient analysis of induction motors in the phase domain could improve the accuracy of such programs by operating in the same domain (i.e. phase domain) as transmission lines and other system components.

In this thesis the magnetic circuit of the induction machine is considered to be linear. However, it is known that this is not actually the case, and that the motor undergoes some degree of saturation which gives rise to a circuit which has non-linear characteristics. The modelling of saturation effects in induction motors using the conventional dq0 coordinates

is quite complex. It is believed that a transient model of the induction machine in the phase domain will present a much simpler and more accurate method for representing saturation.

1.3 Research objectives

The main object of this research is to develop a phase domain transient model of the squirrel-cage induction motor that accurately represents the physical phenomena. The model must also be capable of accurately reflecting steady-state conditions in the motor.

Within the global objective of this thesis there are smaller but not less significant objectives which are of overall importance to the entire project. It was recognised from an early stage that the proposed model for the induction machine would require data not normally given by machine manufacturers. Consequently, there was the task of developing a method that would use the information supplied by the machine manufacturers to obtain data suitable for transient studies with the PDTM. As part of a much larger objective it was established that all programming code must be done with the ADA-95 programming language which offers the possibility of object oriented programming.

Finally, it is hoped that a successful model would lead to a generalisation of the applicability of phase-domain modelling to other electrical apparatus and components of electrical power systems.

Chapter Two

The Induction Machine

2.1 Physical Characteristics

The operating characteristics of most induction machines are fixed at the time they are designed. When construction of the machine is completed there is little that can be done to change its performance characteristics. Although the squirrel-cage induction motor is the subject of this thesis, on many occasions reference will be made to the more general term, induction machine. The design of the machine determines the nominal output, the starting and breakdown torque, the nominal slip and its general steady-state characteristics. These external features common to the user are set by the designer in accordance with his requirement for machine output power and parameters such as the value of the resistances in the stator and rotor windings and the leakage and mutual reactance of both stator and rotor windings. Other factors which determine the characteristics of the machine include the type of magnetic material used in its construction and the combination of width and length of the air gap.

The squirrel-cage induction motor consist of copper wound stator winding to which the supply voltage is connected and a rotor that consist of solid bars of conducting material short circuited at each end and embedded in a ferromagnetic material. The short circuiting of the rotor bars give rise to a common ring which connect all the bars. The

rotor bars of the motor may be cylindrical in shape (single cage rotor), rectangular with greater depth than width in the ferromagnetic alloy (deep-bar rotor), or they may be two separate bars located one above the other with separate end rings (double-cage rotor). In all the above mentioned motors the rotor bars are skewed with respect to the plane of the axis of rotation of the rotor to reduce the magnitude of harmonic torque due to the harmonic content in the magnetomotive force (MMF) waves [2]. Generally, the type of rotor used in the machine depends on the starting and steady state running conditions that are required. Single-cage rotor motors usually have higher starting torques than both double-cage rotor and deep-bar rotors, however, they operate at lower rated velocity and are less efficient [6].

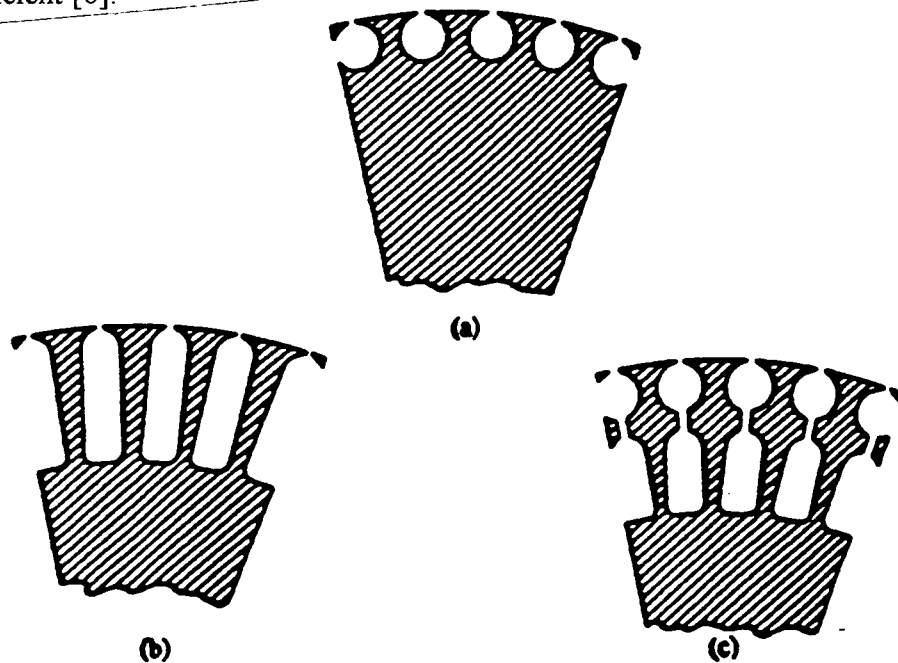


Fig. 1. Squirrel-cage rotor-bar cross sections, (a) single cage, (b) deep-bar and (c) double-cage rotors (NEMA).

2.2 Electromagnetic features of the Induction machine

The basic principle of operation of the induction machine is quite similar to that of a transformer. This is based on the theory of electromagnetic induction. When a three

phase voltage is applied to the stator winding (assume a two pole motor) of the induction machine a rotating magnetic field referred to as the magnetomotive (MMF) field is set up across the air-gap between the stator and the rotor. The speed of rotation (synchronous speed, ω_s) of the MMF is dependent on the frequency (f) of the applied voltage and the number of poles (p) in the stator. The synchronous speed is found from the expression

$$\omega_s = \frac{4\pi f}{p} \text{ Rad./sec.} \quad (2.2.1)$$

The strength of the resulting magnetic field (F) is directly proportional to the effective turns per phase in the stator windings and rms value of the stator phase current (I_s), and inversely proportional to the number of poles. This is expressed by

$$F = \frac{N_{se} I_s}{p} \text{ Amp/pole.} \quad (2.2.2)$$

The rotating magnetic field created by the stator current crosses the air-gap of the machine and sets up a mutual flux linking the stator and rotor. This mutual flux across the air-gap induces a voltage in the rotor conductors. In the squirrel cage motor the rotor conductors are short-circuited and therefore a current flows. The current in the rotor conductors sets up its own magnetic field which interacts with that produced from the stator to give a resultant rotating MMF and a torque in the direction of the movement of the rotor. If we assume a two pole machine, then the combination of stator three phase windings will produce a north and a south pole in the stator which would be mirrored by a north and south pole and an equivalent three phase circuit in the rotor (fig. 2). In the squirrel cage induction motor there are no clearly defined rotor circuit windings. Thus, the effective turns ratio (K) is defined as the relationship between the effective turns per phase of the stator windings (N_{sc}) and the rotor circuit (N_{re}).

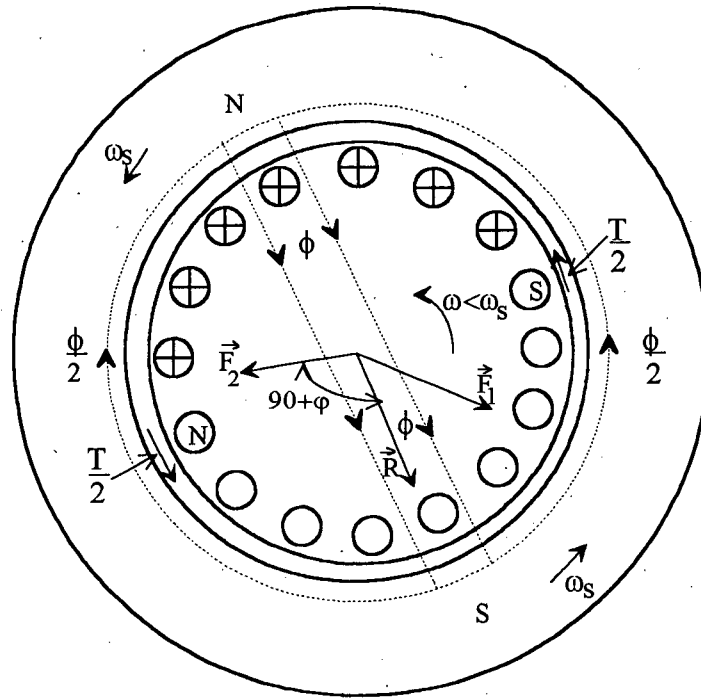


Fig. 2. Magnetic characteristics of a loaded two pole induction motor.

2.3 Induction Machine Circuits

The induction machine can be considered as consisting of two separate electrical circuits (stator and rotor) electromagnetically connected across the air-gap. The stator circuit represents the resistance and self inductance of the phases along with the mutual inductance between phases. Similarly, the rotor circuit represent the resistance and self inductance in each phase as well as the mutual inductance between phases. The magnetising inductance between stator and rotor produces the magnetic link between these two circuits. Although not directly considered in transient studies of the induction motor there are other factors such as air-gap length and width, and the magnetic properties of the iron core that determine the electromagnetic characteristics of the

machine and ultimately its electrical parameters. These are normally considered in the design stages of the motor.

Although we are considering a linear magnetic circuit for the induction motor it is important to mention that saturation occurs and this affects the transient response of the motor. The permeability of the ferromagnetic alloy is finite, and as the current in the circuits increases parts of the leakage and mutual inductance saturates. Saturation of the magnetic circuit causes a slight reduction in the values of the leakage and mutual inductance.

The electrical circuits (stator and rotor) of the wound rotor induction machine are clearly distinguishable and are connected in wye or delta. In normal circumstances one of these circuits is connected in delta [5]. The stator windings in the squirrel-cage induction machine is similar to that in the wound rotor machine, but their rotor windings are different. Nevertheless, the rotor circuit in the squirrel-cage machine like that of the wound rotor machine can be considered to be connected in wye or delta. In the analysis that follows it will be assumed that each phase of the stator and rotor circuits is made up of a winding of several turns and that both stator and rotor windings are connected in wye (fig. 3). The windings of the stator and rotor circuits in figure 3 are both sinusoidally distributed and displaced 120 degrees with identical phase resistance and self inductance in each of the respective circuits.

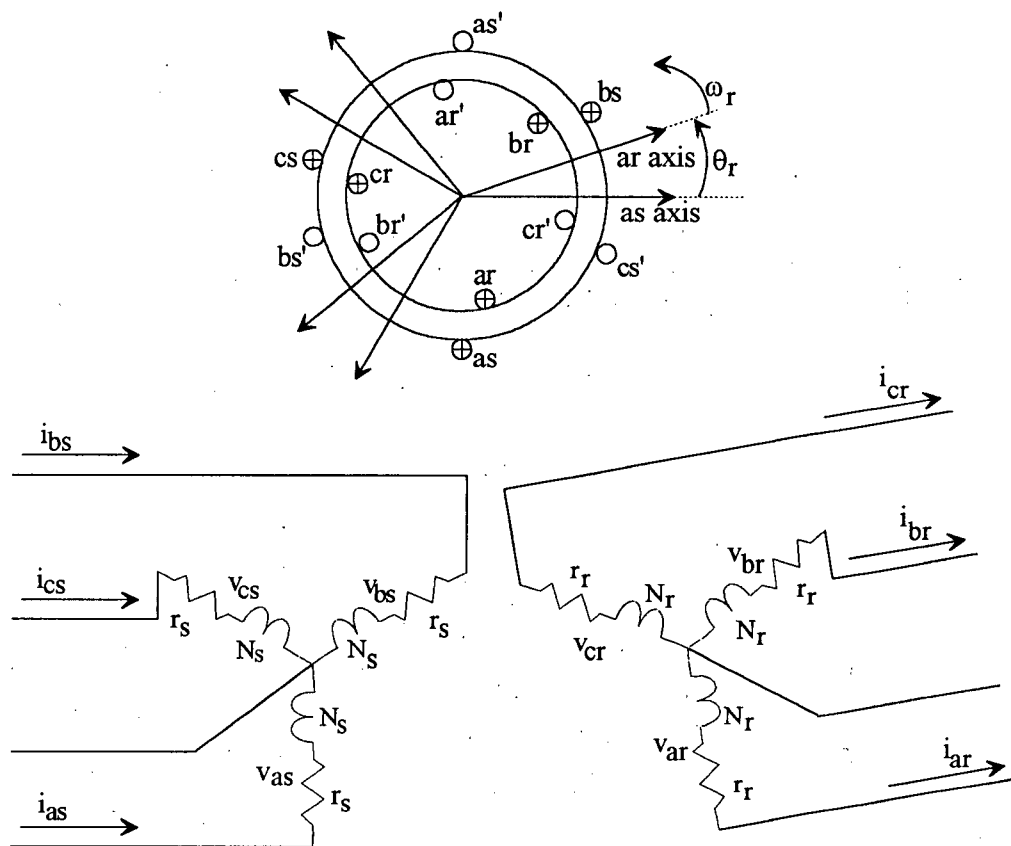


Fig. 3. A two-pole, wye-connected symmetrical induction motor.

The self inductance of the stator is made up of its leakage and magnetising inductance. The leakage inductance usually accounts for approximately 5 to 10 percent of the total self inductance [2]. Both the stator (L_s) and rotor (L_r) self inductances can be represented as

$$L_s = L_{ls} + L_{ms} \quad (2.3.1)$$

$$L_r = L_{lr} + L_{mr} \quad (2.3.2)$$

where L_{ls} and L_{lr} are the leakage inductances, and L_{ms} and L_{mr} are the magnetising inductances of the stator and rotor windings respectively. The magnetising inductance of the stator winding depend on the number of turns in its windings (N_s) as well as some

physical machine parameters and the type of magnetic material. The magnetising inductance of the stator is expressed as

$$L_{ms} = \left(\frac{N_s}{2}\right)^2 \frac{\pi\mu_0 r l}{g} \quad (2.3.3)$$

where μ_0 is the magnetic constant, r is the internal radius of the stator, l is the axial length of the air-gap and g the length of the uniform portion of the air-gap. The magnetising inductance of the rotor windings can also be expressed as

$$L_{mr} = \left(\frac{N_r}{2}\right)^2 \frac{\pi\mu_0 r l}{g} \quad (2.3.4)$$

The mutual inductances between the respective phases of the stator and rotor windings are

$$L_{MS} = -\frac{1}{2}L_{ms} \quad (2.3.5)$$

$$L_{MR} = -\frac{1}{2}L_{mr} \quad (2.3.6)$$

The variables L_{MS} and L_{MR} are the mutual inductances of the stator and rotor windings respectively. From the preceding expressions the inductance matrix of the stator windings (L_{ST}) in a three phase induction machine is

$$[L_{ST}] = \begin{bmatrix} L_{ls} + L_{ms} & -\frac{1}{2}L_{ms} & -\frac{1}{2}L_{ms} \\ -\frac{1}{2}L_{ms} & L_{ls} + L_{ms} & -\frac{1}{2}L_{ms} \\ -\frac{1}{2}L_{ms} & -\frac{1}{2}L_{ms} & L_{ls} + L_{ms} \end{bmatrix} \quad (2.3.7)$$

Similarly, the inductance matrix of the rotor windings (L_{RO}) can be expressed as

$$[L_{RO}] = \begin{bmatrix} L_{lr} + L_{mr} & -\frac{1}{2}L_{mr} & -\frac{1}{2}L_{mr} \\ -\frac{1}{2}L_{mr} & L_{lr} + L_{mr} & -\frac{1}{2}L_{mr} \\ -\frac{1}{2}L_{mr} & -\frac{1}{2}L_{mr} & L_{lr} + L_{mr} \end{bmatrix} \quad (2.3.8)$$

The mutual inductance between stator and rotor circuits expresses the magnetic flux linking these parts of the machine. This mutual inductances between stator and rotor windings (L_{sr}) vary with the position of the rotor and in the case of a three phase induction machine the inductance matrix (L_{SR}) can be expressed as

$$[L_{SR}] = L_{sr} \begin{bmatrix} \cos(\theta_r) & \cos\left(\theta_r + \frac{2\pi}{3}\right) & \cos\left(\theta_r - \frac{2\pi}{3}\right) \\ \cos\left(\theta_r - \frac{2\pi}{3}\right) & \cos(\theta_r) & \cos\left(\theta_r + \frac{2\pi}{3}\right) \\ \cos\left(\theta_r + \frac{2\pi}{3}\right) & \cos\left(\theta_r - \frac{2\pi}{3}\right) & \cos(\theta_r) \end{bmatrix} \quad (2.3.9)$$

where θ_r is the electrical angular position of the rotor and L_{sr} is the amplitude of the mutual inductance. The amplitude of the mutual inductance between the stator and the rotor windings is associated to the stator magnetising inductance as shown in the following expression

$$L_{sr} = \frac{N_r}{N_s} L_{ms} \quad (2.3.10)$$

where N_r and N_s are the effective turns per phase in the rotor and stator windings.

The model that has been described thus far is representative of the single-cage induction motor or the wound rotor motor. The equivalent circuit for this type of motor (fig. 4) was developed by Charles Steinmetz and it forms the basis for all subsequent induction motor equivalent circuit models. This model can be used for transient studies of wound rotor motors and small single-cage motors where the rotor circuit phase current is small.

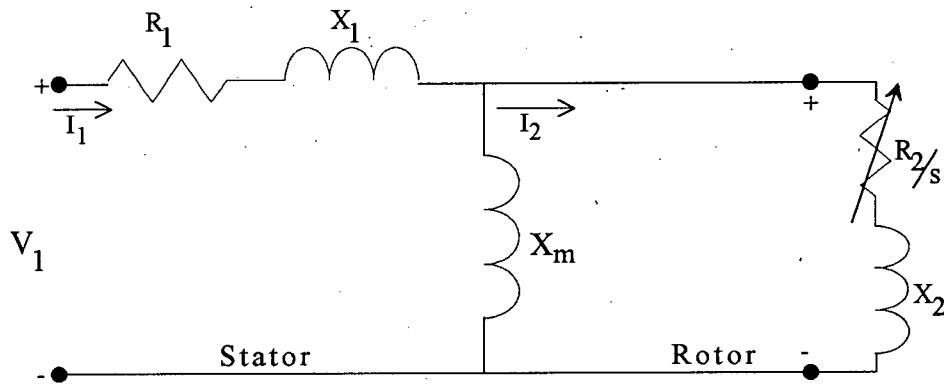


Fig. 4. Steinmetz single phase equivalent circuit of a three phase induction motor

In medium and large size induction machines the rotor current is relatively high and the rotor bar construction is either the double-cage or the deep-bar configuration. In both of these rotor types the effective resistance of the rotor bar changes with rotor speed due to the phenomena referred to as skin effect. The equivalent circuit model in figure 5 shows the rotor represented as two circuits.

In the case of the deep-bar rotor and the double-cage rotor induction motors it has been determined that it is not sufficiently accurate to represent transient phenomena by one rotor circuit. Therefore, these machines should be modelled as two rotor circuits with their own resistances and self inductances (fig. 5). The two rotor circuits representing the deep-bar rotor or the double-cage rotor are connected in parallel. When the induction motor is modelled as two rotor circuits in the phase domain, an extension can be made to the general theoretical formulation made for the single cage or wound rotor machine. In such cases there is mutual inductance between the rotor circuits and the mutual inductance between the stator and rotor takes into account both rotor circuits.

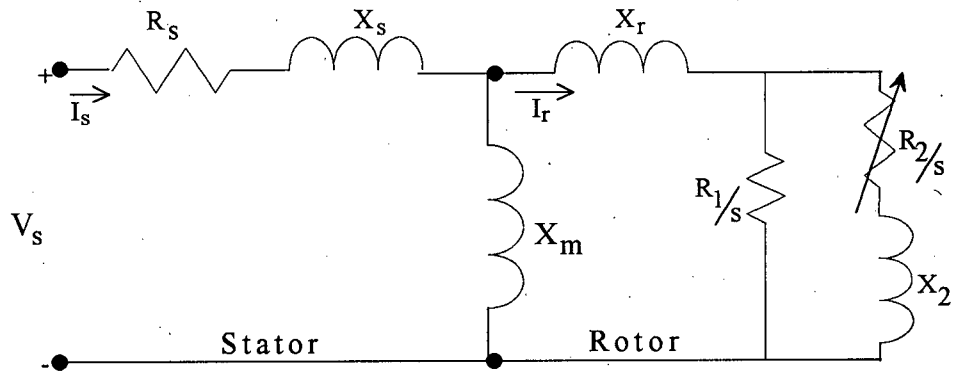


Fig. 5. Equivalent single phase circuit of a three phase induction motor used in transient studies

Chapter Three

The Phase Domain Model Of The Squirrel Cage Induction Motor

In this chapter we will obtain the differential equations for the phase voltages of both stator and rotor circuits. These equations will have time varying mutual inductances caused by the relative motion between stator and rotor circuits. The solution method is based on the discretization of the first order differential equations by means of the trapezoidal rule of integration [10]. This method converts the time varying inductances and other inductances into equivalent resistances and history voltage sources. Consequently, the stator and rotor circuits with their phase resistances, self inductances and mutual inductances are converted into a similar network with only equivalent resistances and voltage sources. A system of equation representing the stator and rotor phase voltages is subsequently developed from the equivalent network of the stator and rotor circuits. This system of equation forms the basis for the solution of the new model in the phase domain

3.1 Solution Technique

The circuit components for the development of the new transient model in the phase domain of the induction motor is the resistor and the inductor. An essential part of the formulation of the model is the solution of the first order differential equation that represents the voltage in self and mutual inductances. The basic expression for the voltage in an inductor is as follows

$$V(t) = L \frac{dI(t)}{dt} \quad (3.1.1)$$

When the trapezoidal rule of integration is used to solve this differential equation we obtain

$$V(t) = \frac{2L}{\Delta t} I(t) - \frac{2L}{\Delta t} I(t - \Delta t) - V(t - \Delta t) \quad (3.1.2)$$

This expression gives the voltage in the inductor at any instant in time denoted by "t". The discretized equation of the voltage has a voltage component in time "t" and a history component ($V_h(t)$) shown in equation (3.1.3). Physically, equation 3.1.2 is demonstrated in figure 6b.

$$V_h(t) = \frac{2L}{\Delta t} I(t - \Delta t) + V(t - \Delta t) \quad (3.1.3)$$

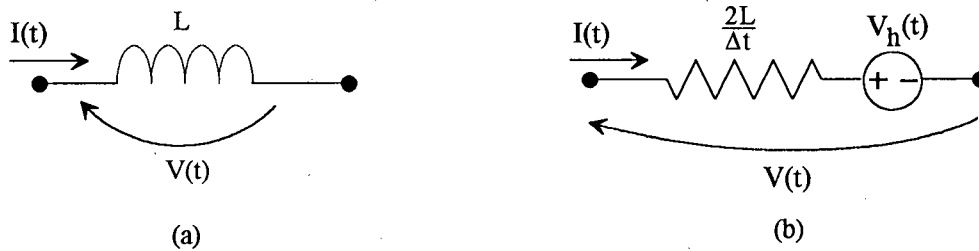


Fig. 6. Voltage in an inductor in (a) continuous-time and (b) discrete time domains.

In the case where a resistor is connected in series with an inductor (fig. 7) it is sometimes desirable to use the voltage across the entire branch instead of just the inductor. In such cases the differential equation for the voltage across the branch is the following:

$$V(t) = RI(t) + L \frac{dI(t)}{dt} \quad (3.1.4)$$

When this first order differential equation is solved by the trapezoidal rule of integration it gives the voltage in every time instant "t" across the branch by the expression (3.1.5).

This expression also has a history voltage component ($V_{hr}(t)$) shown in fig. 7(b), and whose expression is given in (3.1.6).

$$V(t) = RI(t) + \frac{2L}{\Delta t}I(t) + RI(t - \Delta t) - \frac{2L}{\Delta t}I(t - \Delta t) - V(t - \Delta t) \quad (3.1.5)$$

$$V_{hr}(t) = \left[R - \frac{2L}{\Delta t} \right] I(t - \Delta t) - V(t - \Delta t) \quad (3.1.6)$$

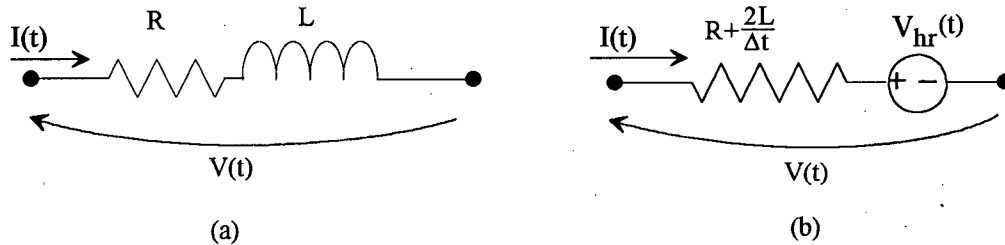


Fig. 7. Voltage across a series resistor-inductor branch in continuous and discrete time domains.

The phases in the stator and rotor circuits of the induction motor model are represented by branches with a resistor in series with an inductor. From the preceding equations one can also recognise the transformation of the inductor to an equivalent resistance (R_{eq}), as in the following expression

$$R_{eq} = \frac{2L}{\Delta t} \quad (3.1.7)$$

where L is the inductance in Henry and Δt is the size of the time step used to discretize the inductance.

3.2 The Stator Circuit

The assumption is made that the stator circuit is connected in wye and that each phase contains a resistor connected in series with an inductor (fig. 8). In this initial analysis the stator circuit will be interpreted as if it were isolated from the rest of the machine. Consequently, the equation representing the phase voltages will reflect only the phase

resistance along with the self and mutual inductances between the phases of the stator. In reality it is known that the stator phase voltages also depend on the magnetic coupling between the stator and rotor windings, this effect will be incorporated to our analysis when we look at the entire machine.

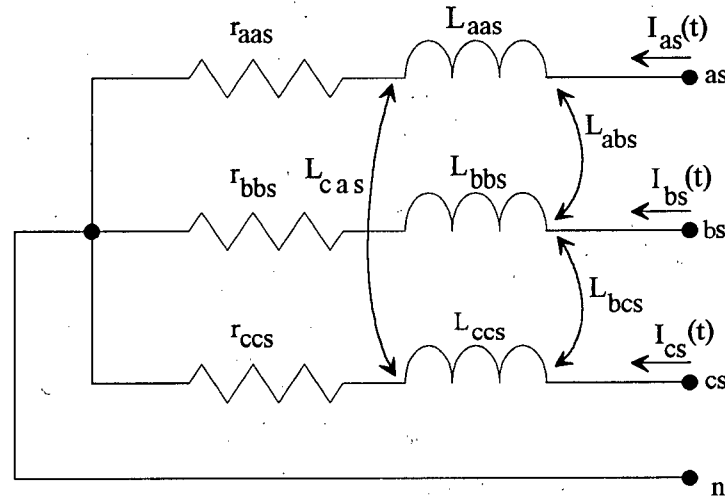


Fig. 8. Stator circuit showing series elements and mutual coupling between phases.

The differential equations representing the voltage in the respective phases of the stator are as follows:

$$V_{as}(t) = r_{aas}I_{as}(t) + L_{aas}\frac{dI_{as}(t)}{dt} + L_{abs}\frac{dI_{bs}(t)}{dt} + L_{acs}\frac{dI_{cs}(t)}{dt} \quad (3.2.1)$$

$$V_{bs}(t) = r_{bbs}I_{bs}(t) + L_{bbs}\frac{dI_{bs}(t)}{dt} + L_{bas}\frac{dI_{as}(t)}{dt} + L_{bcs}\frac{dI_{cs}(t)}{dt} \quad (3.2.2)$$

$$V_{cs}(t) = r_{ccs}I_{cs}(t) + L_{ccs}\frac{dI_{cs}(t)}{dt} + L_{cbs}\frac{dI_{bs}(t)}{dt} + L_{cas}\frac{dI_{as}(t)}{dt} \quad (3.2.3)$$

In matrix form the above equations are transformed to give

$$\begin{bmatrix} V_{as}(t) \\ V_{bs}(t) \\ V_{cs}(t) \end{bmatrix} = \begin{bmatrix} r_{aas} & 0 & 0 \\ 0 & r_{bbs} & 0 \\ 0 & 0 & r_{ccs} \end{bmatrix} * P \begin{bmatrix} L_{aas} & L_{abs} & L_{acs} \\ L_{bas} & L_{bbs} & L_{bcs} \\ L_{cas} & L_{cbs} & L_{ccs} \end{bmatrix} \begin{bmatrix} I_{as}(t) \\ I_{bs}(t) \\ I_{cs}(t) \end{bmatrix} \quad (3.2.4)$$

The differential equations (3.2.1 - 3.2.3) are solved in the time domain to give the expressions (3.2.5) to (3.2.7) for the phase voltages of the stator circuit.

$$V_{as}(t) = \left(r_{aas} + \frac{2}{\Delta t} L_{aas} \right) I_{as}(t) + \frac{2}{\Delta t} L_{abs} I_{bs}(t) + \frac{2}{\Delta t} L_{acs} I_{cs}(t) + \left(r_{aas} - \frac{2}{\Delta t} L_{aas} \right) I_{as}(t - \Delta t) \\ - \frac{2}{\Delta t} L_{abs} I_{bs}(t - \Delta t) - \frac{2}{\Delta t} L_{acs} I_{cs}(t - \Delta t) - V_{as}(t - \Delta t) \quad (3.2.5)$$

$$V_{bs}(t) = \left(r_{bbs} + \frac{2}{\Delta t} L_{bbs} \right) I_{bs}(t) + \frac{2}{\Delta t} L_{bas} I_{as}(t) + \frac{2}{\Delta t} L_{bcs} I_{cs}(t) + \left(r_{bbs} - \frac{2}{\Delta t} L_{bbs} \right) I_{bs}(t - \Delta t) \\ - \frac{2}{\Delta t} L_{bas} I_{as}(t - \Delta t) - \frac{2}{\Delta t} L_{bcs} I_{cs}(t - \Delta t) - V_{bs}(t - \Delta t) \quad (3.2.6)$$

$$V_{cs}(t) = \left(r_{ccs} + \frac{2}{\Delta t} L_{ccs} \right) I_{cs}(t) + \frac{2}{\Delta t} L_{cas} I_{as}(t) + \frac{2}{\Delta t} L_{cbs} I_{bs}(t) + \left(r_{ccs} - \frac{2}{\Delta t} L_{ccs} \right) I_{cs}(t - \Delta t) \\ - \frac{2}{\Delta t} L_{cas} I_{as}(t - \Delta t) - \frac{2}{\Delta t} L_{cbs} I_{bs}(t - \Delta t) - V_{cs}(t - \Delta t) \quad (3.2.7)$$

The matrix form of these equations is;

$$\begin{bmatrix} V_{as}(t) \\ V_{bs}(t) \\ V_{cs}(t) \end{bmatrix} = \begin{bmatrix} r_{aas} & 0 & 0 \\ 0 & r_{bbs} & 0 \\ 0 & 0 & r_{ccs} \end{bmatrix} + \begin{bmatrix} \frac{2}{\Delta t} L_{aas} & \frac{2}{\Delta t} L_{abs} & \frac{2}{\Delta t} L_{acs} \\ \frac{2}{\Delta t} L_{bas} & \frac{2}{\Delta t} L_{bbs} & \frac{2}{\Delta t} L_{bcs} \\ \frac{2}{\Delta t} L_{cas} & \frac{2}{\Delta t} L_{cbs} & \frac{2}{\Delta t} L_{ccs} \end{bmatrix} \begin{bmatrix} I_{as}(t) \\ I_{bs}(t) \\ I_{cs}(t) \end{bmatrix} + \begin{bmatrix} E_{ash}(t) \\ E_{bsh}(t) \\ E_{csh}(t) \end{bmatrix} \quad (3.2.8)$$

where $E_{ash}(t)$, $E_{bsh}(t)$ and $E_{csh}(t)$ are the history voltage sources in phases a, b and c of the stator circuit. In this case

$$E_{ash}(t) = \left(r_{aas} - \frac{2}{\Delta t} L_{aas} \right) I_{as}(t - \Delta t) - \frac{2}{\Delta t} L_{abs} I_{bs}(t - \Delta t) - \frac{2}{\Delta t} L_{acs} I_{cs}(t - \Delta t) - V_{as}(t - \Delta t) \quad (3.2.9)$$

$$E_{bsh}(t) = \left(r_{bbs} - \frac{2}{\Delta t} L_{bbs} \right) I_{bs}(t - \Delta t) - \frac{2}{\Delta t} L_{bas} I_{as}(t - \Delta t) - \frac{2}{\Delta t} L_{bcs} I_{cs}(t - \Delta t) - V_{bs}(t - \Delta t) \quad (3.2.10)$$

$$E_{csh}(t) = \left(r_{ccs} - \frac{2}{\Delta t} L_{ccs} \right) I_{cs}(t - \Delta t) - \frac{2}{\Delta t} L_{cas} I_{as}(t - \Delta t) - \frac{2}{\Delta t} L_{cbs} I_{bs}(t - \Delta t) - V_{cs}(t - \Delta t) \quad (3.2.11)$$

In these equations the value of the phase currents in " $(t-\Delta t)$ " represent the history value of these currents in the respective phases.

The system of equations in matrix form shown in (3.2.8) can be written in compact notation as

$$[V_s(t)] = [RL_s][I_s(t)] + [E_{sh}(t)] \quad (3.2.12)$$

where

$$[RL_s] = [[R_s] + [L_s]] \quad (3.2.13)$$

The discretization of the differential equations for the stator voltage allows us to obtain the discrete-time equivalent circuit for the stator windings shown in fig. 9. The self and mutual inductances in the equations (3.2.1) to (3.2.3) have been all converted to equivalent resistances.

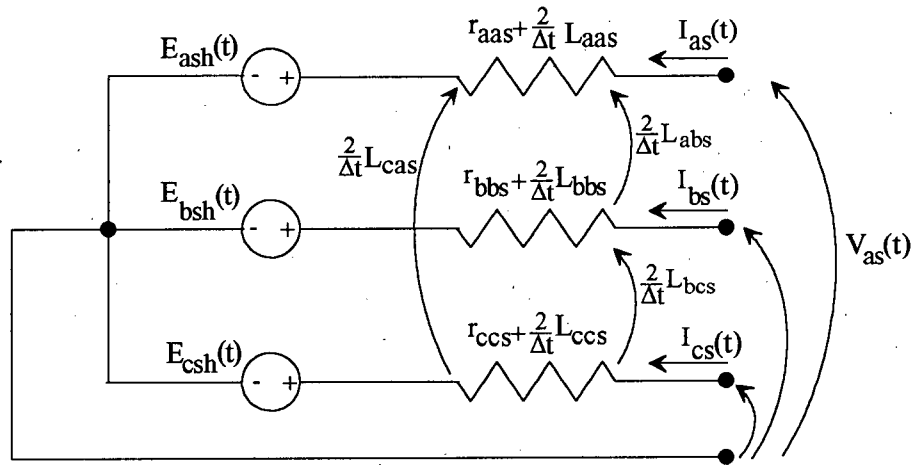


Fig. 9. Discrete-time equivalent circuit of the stator windings.

3.3 The Rotor Circuits

Although the emphasis in this thesis has been on the development of a model for the deep-bar and double-cage induction machine, a program has also been developed for the simulation of the single-cage rotor machine. However, these machines are generally of small power output and therefore are not normally the focus of transient studies. In an effort to uncover what may not be quite evident the analysis of the rotor circuits will concentrate on the deep-bar rotor and then make the necessary extensions to the double cage rotor.

The shape of the deep-bar rotor in the squirrel-cage induction motor (fig. 10) gives rise to a nonuniform distribution of current in the bars during transient or changing rotor speed. This unequal distribution of current, coupled with the difference in reluctance between the magnetic material and the air in the machine air gap, causes a variation in flux as one moves from the outer to the inner portion of the rotor-bar. These factors combine to create a larger leakage inductance in the inner part of the bar than on the outer portion of the bar. That portion of the rotor bar referred to as the outer portion forms one rotor circuit while the other portion forms the inner rotor circuit (rotor circuit one and rotor circuit two, respectively). It is quite evident that there really is no clear physical separation between the two circuit as in a double-cage machine.

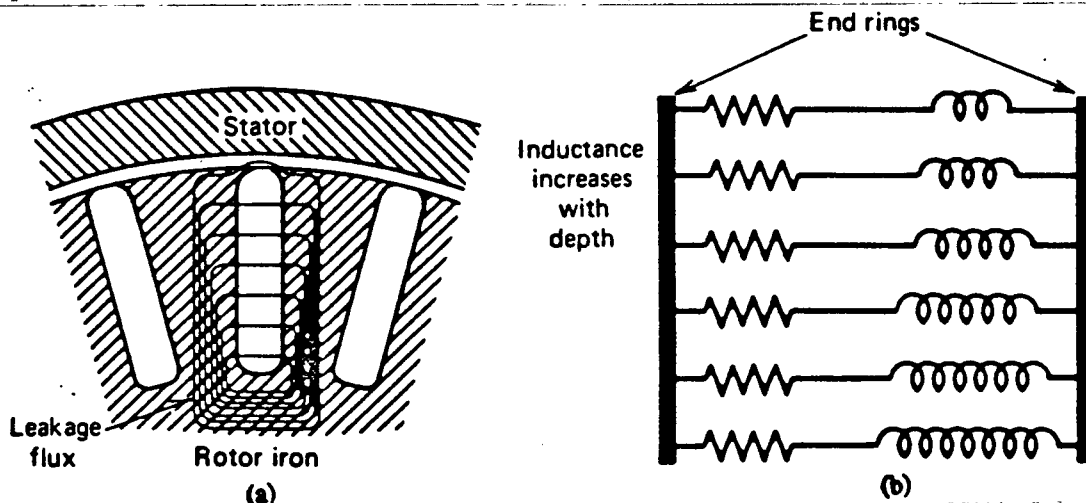


Fig. 10. Deep-bar rotor effects. (a) Leakage flux paths. (b) circuit representation showing varying inductance.

In the two circuit representation of the deep-bar rotor motor the resistance of the outer circuit is higher than that of the inner circuit and the leakage inductance of the former is so small that it is normally not considered. In the double-cage rotor machine the leakage inductance of the outer circuit is also small, although some researchers claim that its value can be between 5 to 20 percent of the value of the mutual inductance between the two rotor circuits. The value of this leakage inductance is closer to the upper limits of this range when separate end rings and different axial extensions beyond the core ends of the two cages are used in machine design [11]. In this thesis a general model has been

developed which would allow for the utilisation of a value for the leakage inductance of the outer circuit if the analyst using the program determine that it is necessary.

In the analysis of the rotor circuits we will first analyse one of the circuits and then show the interrelationship between them. It is again assumed that the rotor "windings" are connected in wye and are initially considered to be in open circuit (fig 11).

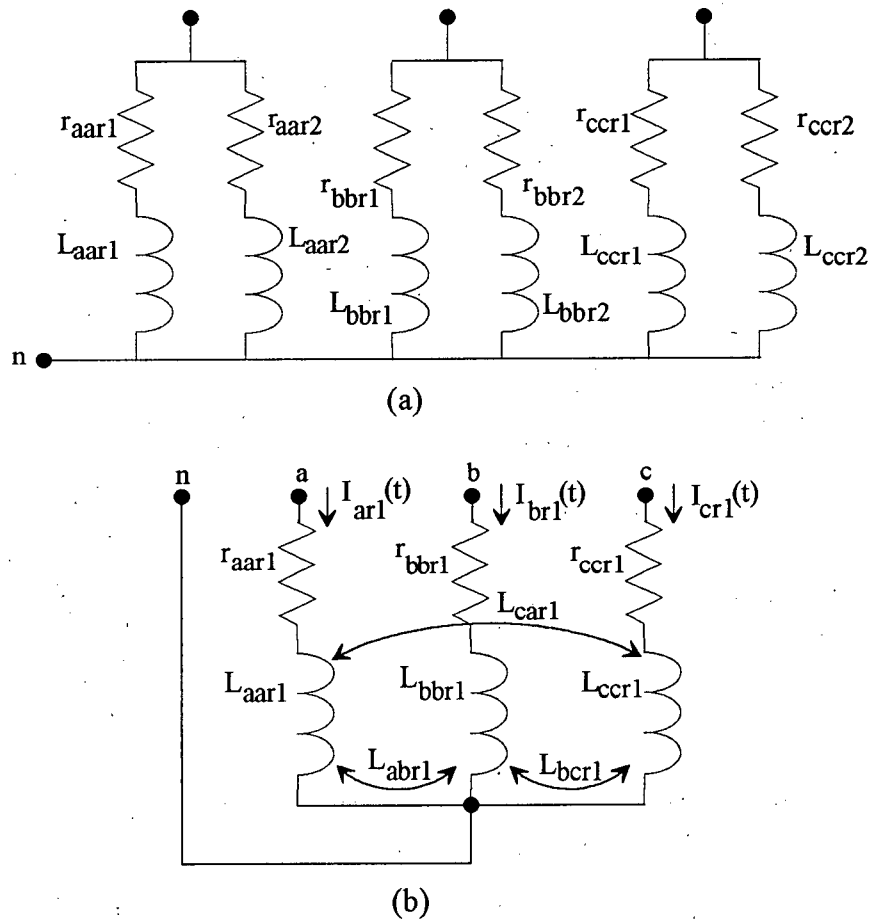


Fig. 11. Rotor equivalent circuit. (a) Two rotor circuits in parallel. (b) Rotor circuit one (not short-circuited).

Rotor circuit one in fig. 11(b) is identical to that shown for the stator windings. The resistance and self inductance in phases a, b and c are all equal, as well as the mutual inductance between the phases. Consequently, the differential equations for the phase voltages in rotor circuit one will be as follows:

$$V_{ar1}(t) = r_{aar1}I_{ar1}(t) + L_{aar1}\frac{dI_{ar1}(t)}{dt} + L_{abr1}\frac{dI_{br1}(t)}{dt} + L_{acr1}\frac{dI_{cr1}(t)}{dt} \quad (3.3.1)$$

$$V_{br1}(t) = r_{bbr1}I_{br1}(t) + L_{bbr1}\frac{dI_{br1}(t)}{dt} + L_{bar1}\frac{dI_{ar1}(t)}{dt} + L_{bcr1}\frac{dI_{cr1}(t)}{dt} \quad (3.3.2)$$

$$V_{cr1}(t) = r_{ccr1}I_{cr1}(t) + L_{ccr1}\frac{dI_{cr1}(t)}{dt} + L_{cbr1}\frac{dI_{br1}(t)}{dt} + L_{car1}\frac{dI_{ar1}(t)}{dt} \quad (3.3.3)$$

In equations (3.3.1) to (3.3.3) the voltage in each phase of the rotor winding depends on its resistance, self inductance and the mutual inductance between phases. The solution of the first order differential equations of the voltages can be expressed as

$$\begin{bmatrix} V_{ar1}(t) \\ V_{br1}(t) \\ V_{cr1}(t) \end{bmatrix} = \begin{bmatrix} r_{aar1} & 0 & 0 \\ 0 & r_{bbr1} & 0 \\ 0 & 0 & r_{ccr1} \end{bmatrix} + \begin{bmatrix} \frac{2}{\Delta t}L_{aar1} & \frac{2}{\Delta t}L_{abr1} & \frac{2}{\Delta t}L_{acr1} \\ \frac{2}{\Delta t}L_{bar1} & \frac{2}{\Delta t}L_{bbr1} & \frac{2}{\Delta t}L_{bcr1} \\ \frac{2}{\Delta t}L_{car1} & \frac{2}{\Delta t}L_{cbr1} & \frac{2}{\Delta t}L_{ccr1} \end{bmatrix} \begin{bmatrix} I_{ar1}(t) \\ I_{br1}(t) \\ I_{cr1}(t) \end{bmatrix} + \begin{bmatrix} E_{ar1h}(t) \\ E_{br1h}(t) \\ E_{cr1h}(t) \end{bmatrix} \quad (3.3.4)$$

where $E_{ar1h}(t)$, $E_{br1h}(t)$ and $E_{cr1h}(t)$ are the history voltage sources in each phase of rotor circuit one. The equation form of the history voltage sources in the rotor circuit is similar to that shown in the expressions 3.2.9 - 3.2.11 for the stator windings. The system of equations in (3.3.4) can be expressed in compact form as

$$[V_{r1}(t)] = [RL_{r1}][I_{r1}(t)] + [E_{r1h}(t)] \quad (3.3.5)$$

with

$$[RL_{r1}] = [[R_{r1}] + [L_{r1}]] \quad (3.3.6)$$

The discretized equations in expression 3.3.4 for rotor one circuit can be represented by the equivalent circuit in figure 12.

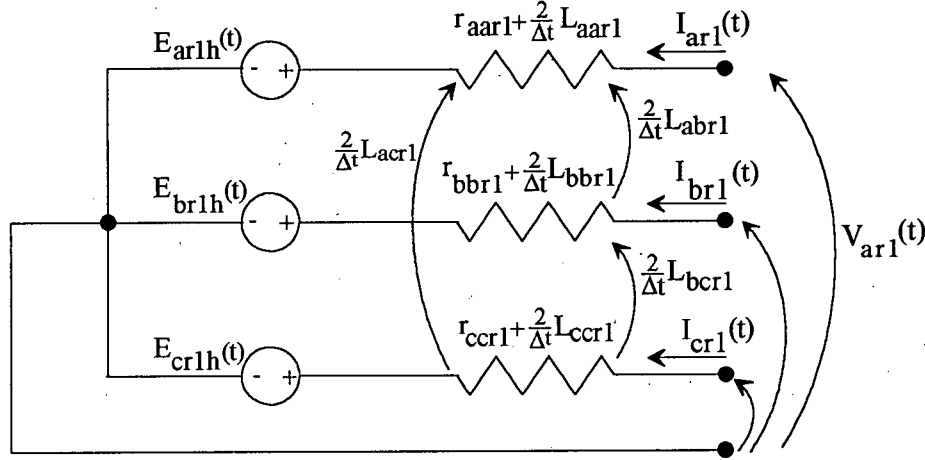


Fig. 12. Discretized equivalent circuit of the rotor windings.

Both rotor circuits of the induction motor are identical except for the values of their components. Therefore, the discretize equation for the phase voltages in rotor circuit two can be expressed as

$$\begin{bmatrix} V_{ar2}(t) \\ V_{br2}(t) \\ V_{cr2}(t) \end{bmatrix} = \begin{bmatrix} r_{aar2} & 0 & 0 \\ 0 & r_{bbr2} & 0 \\ 0 & 0 & r_{ccr2} \end{bmatrix} + \begin{bmatrix} \frac{2}{\Delta t} L_{aar2} & \frac{2}{\Delta t} L_{abr2} & \frac{2}{\Delta t} L_{acr2} \\ \frac{2}{\Delta t} L_{bar2} & \frac{2}{\Delta t} L_{bbr2} & \frac{2}{\Delta t} L_{bcr2} \\ \frac{2}{\Delta t} L_{car2} & \frac{2}{\Delta t} L_{cbr2} & \frac{2}{\Delta t} L_{ccr2} \end{bmatrix} \begin{bmatrix} I_{ar2}(t) \\ I_{br2}(t) \\ I_{cr2}(t) \end{bmatrix} + \begin{bmatrix} E_{ar2h}(t) \\ E_{br2h}(t) \\ E_{cr2h}(t) \end{bmatrix} \quad (3.3.7)$$

The system of equations in 3.3.7 can be expressed in compact form as

$$[V_{r2}(t)] = [RL_{r2}][I_{r2}(t)] + [E_{r2h}(t)] \quad (3.3.8)$$

where

$$[RL_{r2}] = [[R_{r2}] + [L_{r2}]] \quad (3.3.9)$$

In our analysis so far we have looked at the machine electrical circuits as completely independent and isolated components whose phase voltage depends only on the series element in each phase and the magnetic coupling between the phases. However, due to

the inductance of both the stator and rotor windings and the ferromagnetic material in which the windings are embedded there is a substantial amount of magnetic coupling between the circuits. Therefore, in the next section we will show how the electromagnetic coupling between the machine windings affect the phase voltages in the stator and rotor circuits.

3.4 The Combined Stator-Rotor Circuit Analysis

In an effort to simplify the analysis of the machine electrical circuits, the phases of the stator and rotor will be considered simply as coils with a determined number of turns (fig. 13). The coils have been separated and placed at 120 degrees with respect to each other and are drawn in a manner to ease the visualization of a wye connection. It is important to bear in mind that while the windings of rotor circuit one and rotor circuit two appear separately, in reality these may represent a single conductor or two conductors with identical position relative to the stator windings.

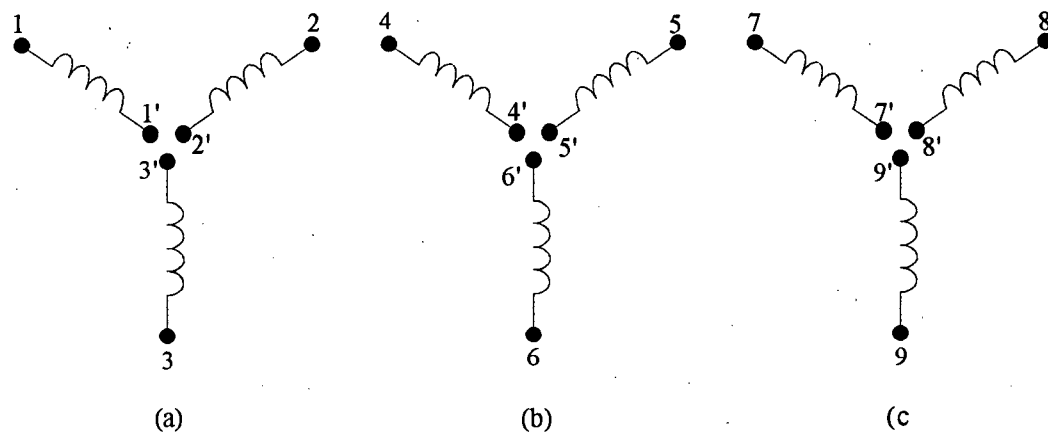


Fig. 13. The phases/windings of (a) the stator circuit, (b) rotor circuit one and (c) rotor circuit two.

In the analysis which follows, stator windings 1-1', 2-2' and 3-3' represent phases a, b and c of the stator circuit, while windings 4-4', 5-5', and 6-6' correspond to phases A1, B1 and C1 of rotor circuit one. Similarly, windings 7-7', 8-8', and 9-9' are representative of phases A2, B2 and C2 of rotor circuit two. The analysis will consider one phase of each

the stator and rotor circuits. The results will be extended to include all three phases of the circuits.

When the machine is energised and the rotor stalled, transformer theory is used to establish a positive sequence equivalent network of the machine (fig. 14) from its representation in figure 13. In equations 3.4.1 to 3.4.3, Z_1 , Z_4 and Z_7 represent the series impedance (i.e. the resistance and the self inductance of each coil) of phases a, A1 and A2 of the three machine circuits in figure 14, and the coil voltages are in effect the phase voltages of one phase of each circuit. The magnetising inductance between the stator and rotor is represented by Z_m . The relative position of the rotor coils 4-4' and 7-7' with respect to the stator coil 1-1' is denoted by the angle theta (θ).

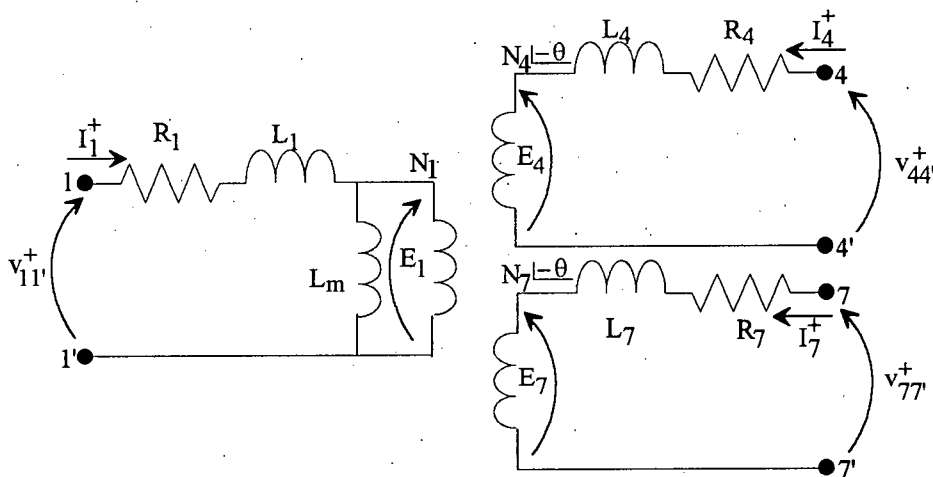


Fig. 14. Positive sequence circuit of one phase of the stator and rotor circuits in the induction motor.

The positive sequence voltage in the respective windings of figure 14 is determined by the following equations:

$$V_{11}' = (Z_1 + Z_m)I_1 + Z_mkI_4 + Z_mkI_7 \quad (3.4.1)$$

$$V_{44}' = kZ_mI_1 + (Z_4 + k^2Z_m)I_4 + k^2Z_m \quad (3.4.2)$$

$$V_{77}' = kZ_mI_1 + k^2Z_mI_4 + (Z_7 + k^2Z_m) \quad (3.4.3)$$

Where $k=N_4/N_1=N_7/N_1$, with N being the number of effective turns per phase in the corresponding machine circuit. Also, all voltages, currents and impedances are represented as phasors. Expressions 3.3.1 - 3.3.3 in matrix format give

$$\begin{bmatrix} V_{11}' \\ V_{44}' \\ V_{77}' \end{bmatrix} = \begin{bmatrix} (Z_1 + Z_m) & kZ_m & kZ_m \\ kZ_m & (Z_4 + k^2Z_m) & k^2Z_m \\ kZ_m & k^2Z_m & Z_7 + k^2Z_m \end{bmatrix} \begin{bmatrix} I_1 \\ I_4 \\ I_7 \end{bmatrix} \quad (3.4.4)$$

It can be seen from 3.3.4 that the positive sequence phase voltage in the respective circuits is a function of their series impedance (i.e. resistance and self inductance) and the magnetic coupling between the windings represented by Z_m .

In the same manner that an equivalent circuit is obtained for the positive sequence voltage it is also possible to deduce the equivalent circuits for the negative and zero sequences (fig. 15). These circuits are then used to obtain the voltage expressions for the negative and zero sequence voltage in the phases of the stator and rotor circuits.

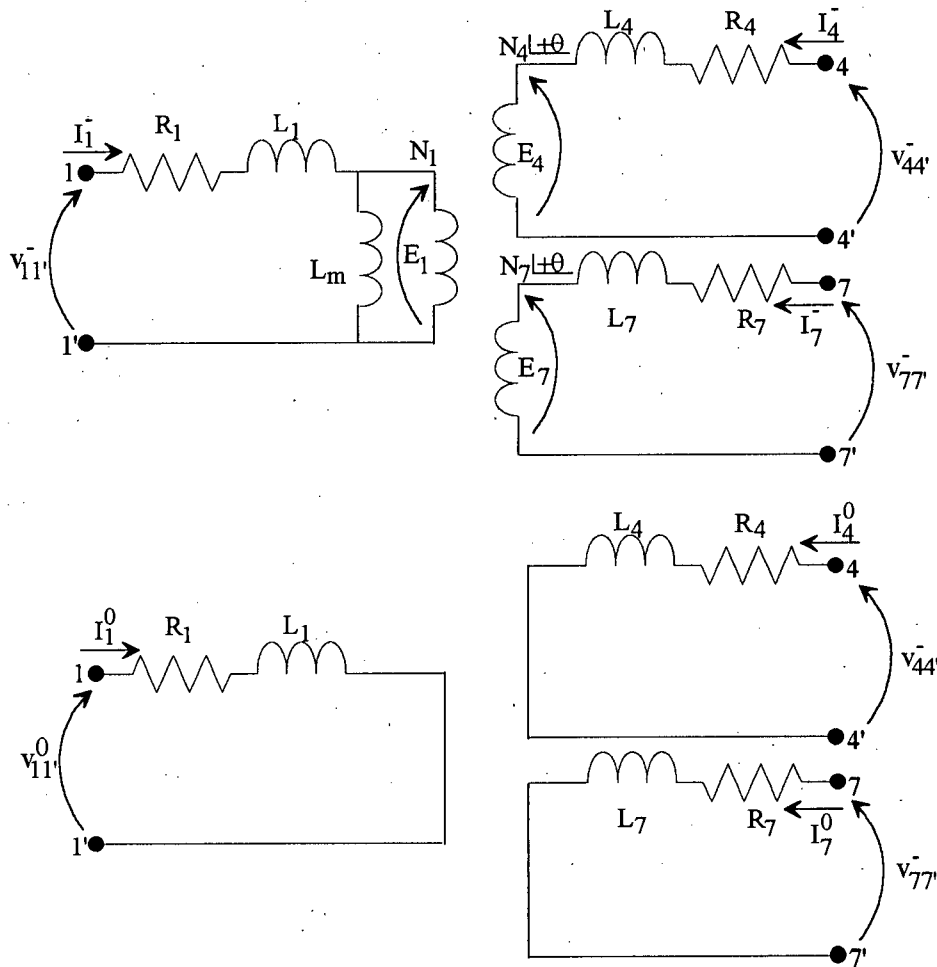


Fig. 15. Negative (a) and zero (b) sequence circuits of stator and rotor circuits in the induction motor.

The expression for the negative sequence voltage is identical to that of the positive sequence voltage. However, the zero sequence voltages in the windings is expressed by

$$\begin{bmatrix} V_{11'}^0 \\ V_{44'}^0 \\ V_{77'}^0 \end{bmatrix} = \begin{bmatrix} Z_1 & 0 & 0 \\ 0 & Z_4 & 0 \\ 0 & 0 & Z_7 \end{bmatrix}^0 \begin{bmatrix} I_1^0 \\ I_4^0 \\ I_7^0 \end{bmatrix} \quad (3.4.5)$$

The three two-port decoupled sequence network (figs. 14 & 15) can be converted by a matrix transformation into three two-port coupled phase-coordinates network of the actual physical device (fig. 16). Combining equation 3.4.4 for the positive and negative

sequence and equation 3.4.5 for the zero sequence mode , the full three-port modal equation is given by

$$\begin{bmatrix} V_{11'}^0 \\ V_{44'}^0 \\ V_{77'}^0 \\ V_{11'}^+ \\ V_{44'}^+ \\ V_{77'}^+ \\ V_{11'}^- \\ V_{44'}^- \\ V_{77'}^- \end{bmatrix} = \begin{bmatrix} [Z^0] & 0 & 0 \\ 0 & [Z^+] & 0 \\ 0 & 0 & [Z^-] \end{bmatrix} \begin{bmatrix} I_{11'}^0 \\ I_{44'}^0 \\ I_{77'}^0 \\ I_{11'}^+ \\ I_{44'}^+ \\ I_{77'}^+ \\ I_{11'}^- \\ I_{44'}^- \\ I_{77'}^- \end{bmatrix} \quad (3.4.6)$$

The corresponding phase-coordinates equation is obtained from

$$[Z_s] = \frac{1}{3}([Z]^0 + 2 \times [Z]^+) \quad (3.4.7)$$

$$[Z_{mu}] = \frac{1}{3}([Z]^0 - [Z]^+) \quad (3.4.8)$$

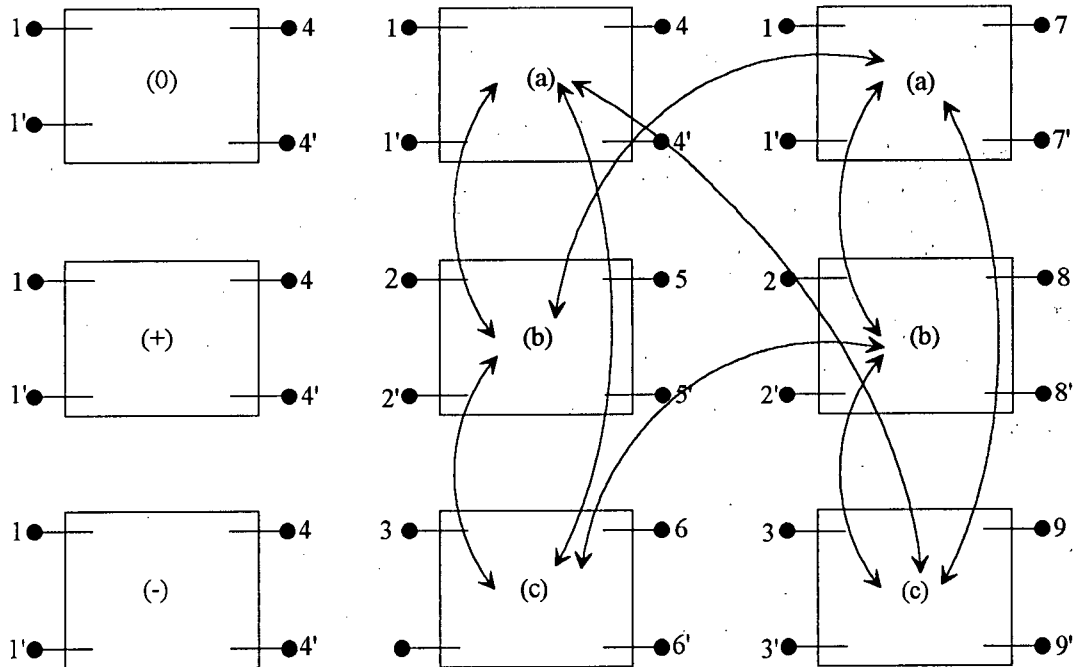


Fig. 16. Conversion from 0-1-2 components (zero, positive and negative sequence) to a-b-c components (actual windings).

The application of 3.4.7 and 3.4.8 to equations 3.4.4 and 3.4.5 gives us the following expressions for the self (Z_s) and mutual (Z_{mu}) impedance matrices

$$[Z_s] = \begin{bmatrix} Z_1 + \frac{2}{3}Z_m & \frac{2}{3}kZ_m & \frac{2}{3}kZ_m \\ \frac{2}{3}kZ_m & Z_4 + \frac{2}{3}k^2Z_m & \frac{2}{3}k^2Z_m \\ \frac{2}{3}kZ_m & \frac{2}{3}k^2Z_m & Z_7 + \frac{2}{3}k^2Z_m \end{bmatrix} \quad (3.4.9)$$

$$[Z_{mu}] = \begin{bmatrix} -\frac{1}{3}Z_m & -\frac{1}{3}kZ_m & -\frac{1}{3}kZ_m \\ -\frac{1}{3}kZ_m & -\frac{1}{3}k^2Z_m & -\frac{1}{3}k^2Z_m \\ -\frac{1}{3}kZ_m & -\frac{1}{3}k^2Z_m & -\frac{1}{3}k^2Z_m \end{bmatrix} \quad (3.4.10)$$

The introduction of the concept of self and mutual impedance matrix extends our analysis from the single phase scenario where there were three windings (one from the stator and one from each of the two rotor circuits) to the real situation with three phases and nine windings (fig. 17).

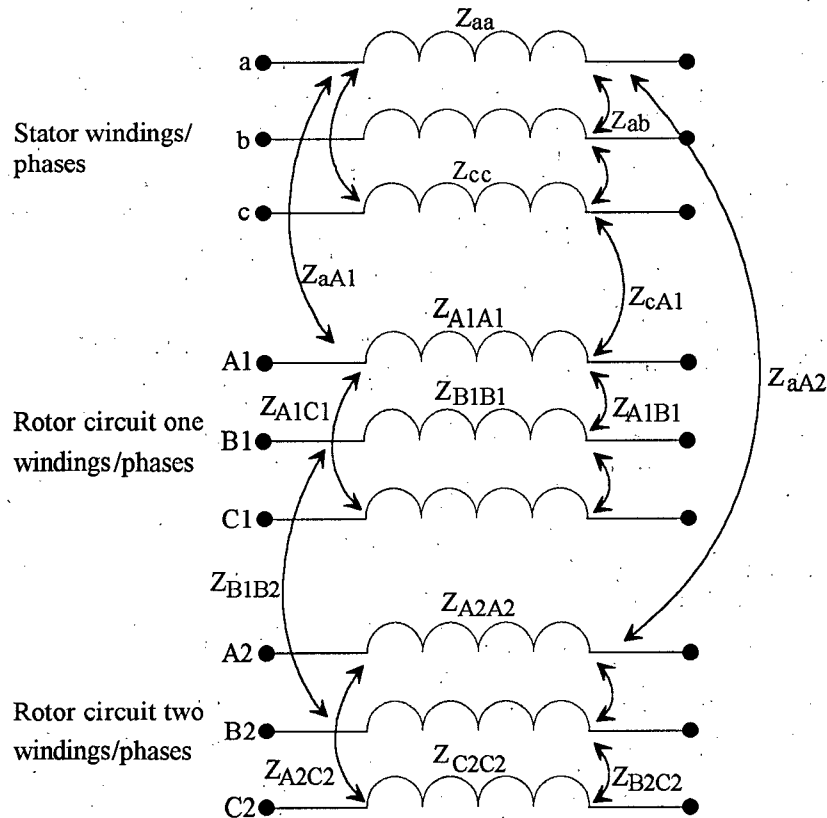


Fig. 17. Magnetic interaction of the stator and rotor circuits of the induction motor.

With the aid of figure 17 and expressions 3.4.7 and 3.4.8 the self and mutual impedance matrix for the three phase network of coupled coils is defined as

$$[Z_s] = \begin{bmatrix} Z_{aa} & Z_{aA1} & Z_{aA2} \\ Z_{A1a} & Z_{A1A1} & Z_{A1A2} \\ Z_{A2a} & Z_{A2A1} & Z_{A2A2} \end{bmatrix} \quad (3.4.11)$$

$$[Z_{mu}] = \begin{bmatrix} Z_{ab} & Z_{aB1} & Z_{aB2} \\ Z_{A1b} & Z_{A1B1} & Z_{A1B2} \\ Z_{A2b} & Z_{A2B1} & Z_{A2B2} \end{bmatrix} \quad (3.4.12)$$

Expressions 3.4.9 and 3.4.10 are then used to obtain the complete impedance matrix of the induction machine. It is now possible to show the voltage in each phase of the three circuits with the magnetic coupling effect included. This is shown in the following expression:

$$\begin{bmatrix} V_a \\ V_b \\ V_c \\ V_{A1} \\ V_{B1} \\ V_{C1} \\ V_{A2} \\ V_{B2} \\ V_{C2} \end{bmatrix} = \begin{bmatrix} Z_{aa} & Z_{ab} & Z_{ab} & Z_{aA1} & Z_{aB1} & Z_{aB1} & Z_{aA2} & Z_{aB2} & Z_{aB2} \\ Z_{ab} & Z_{aa} & Z_{ab} & Z_{aB1} & Z_{aA1} & Z_{aB1} & Z_{aB2} & Z_{aA2} & Z_{aB2} \\ Z_{ab} & Z_{ab} & Z_{aa} & Z_{aB1} & Z_{aB1} & Z_{aA1} & Z_{aB2} & Z_{aB2} & Z_{aA2} \\ Z_{A1a} & Z_{A1b} & Z_{A1b} & Z_{A1A1} & Z_{A1B1} & Z_{A1B1} & Z_{A1A2} & Z_{A1B2} & Z_{A1B2} \\ Z_{A1b} & Z_{A1a} & Z_{A1b} & Z_{A1B1} & Z_{A1A1} & Z_{A1B1} & Z_{A1B2} & Z_{A1A2} & Z_{A1B2} \\ Z_{A1b} & Z_{A1b} & Z_{A1a} & Z_{A1B1} & Z_{A1B1} & Z_{A1A1} & Z_{A1B2} & Z_{A1B2} & Z_{A1A2} \\ Z_{A2a} & Z_{A2b} & Z_{A2b} & Z_{A2A1} & Z_{A2B1} & Z_{A2B1} & Z_{A2A2} & Z_{A2B2} & Z_{A2B2} \\ Z_{A2b} & Z_{A2a} & Z_{A2b} & Z_{A2B1} & Z_{A2A1} & Z_{A2B1} & Z_{A2B2} & Z_{A2A2} & Z_{A2B2} \\ Z_{A2b} & Z_{A2b} & Z_{A2a} & Z_{A2B1} & Z_{A2B1} & Z_{A2A1} & Z_{A2B2} & Z_{A2B2} & Z_{A2A2} \end{bmatrix} \begin{bmatrix} I_a \\ I_b \\ I_c \\ I_{A1} \\ I_{B1} \\ I_{C1} \\ I_{A2} \\ I_{B2} \\ I_{C2} \end{bmatrix} \quad (3.4.13)$$

Where V_a , V_b , V_c , V_{A1} , V_{B1} , V_{C1} , V_{A2} , V_{B2} and V_{C2} represent the phase voltages in the stator, rotor circuit one, and rotor circuit two, respectively. The current vector represent the phase currents of the stator and rotor circuits. Expression 3.4.13 represent all machine parameters in phasor quantities. Matrix expression 3.4.13 is converted to compact form in the time domain as

$$\begin{bmatrix} V_s(t) \\ V_{r1}(t) \\ V_{r2}(t) \end{bmatrix} = \begin{bmatrix} RL_s & L_{sr1} & L_{sr2} \\ L_{r1s} & RL_{r1} & L_{r1r2} \\ L_{r2s} & L_{r2r1} & RL_{r2} \end{bmatrix} \begin{bmatrix} I_s(t) \\ I_{r1}(t) \\ I_{r2}(t) \end{bmatrix} \quad (3.4.14)$$

where

$[V_s(t)]$, $[V_{r1}(t)]$, and $[V_{r2}(t)]$ are the vectors of the stator and rotor phase voltages;

$[I_s(t)]$, $[I_{r1}(t)]$, and $[I_{r2}(t)]$ are the vectors of the stator and rotor phase currents;

$[RL_s]$, $[RL_{r1}]$, and $[RL_{r2}]$ are matrices that reflect the phase resistances as well as the self and mutual inductances between stator phases, rotor circuit one phases and rotor circuit two phases, respectively;

$[L_{sr1}]$ and $[L_{sr2}]$ are the matrices that represent the mutual inductances between stator and rotor circuits; and

$[L_{r1r2}]$ is the matrix of the mutual inductance between the rotor circuits. Also, $[L_{r1s}] = [L_{sr2}]^T$, $[L_{r2s}] = [L_{sr1}]^T$ and $[L_{r2r1}] = [L_{r1r2}]^T$.

By making an analogy between the submatrices in expression 3.4.14 and the equations given in section 2.3 for the self and mutual inductances of coupled windings, the terms of these matrices can be determined. The matrix $[RL_s]$ is as follows

$$[RL_s] = \begin{bmatrix} R_{aas} & 0 & 0 \\ 0 & R_{bbs} & 0 \\ 0 & 0 & R_{ccs} \end{bmatrix} + \begin{bmatrix} L_{ls} + L_{ms} & -\frac{1}{2}L_{ms} & -\frac{1}{2}L_{ms} \\ -\frac{1}{2}L_{ms} & L_{ls} + L_{ms} & -\frac{1}{2}L_{ms} \\ -\frac{1}{2}L_{ms} & -\frac{1}{2}L_{ms} & L_{ls} + L_{ms} \end{bmatrix} \quad (3.4.15)$$

where R_{aas} , R_{bbs} , and R_{ccs} are the resistances in the a, b and c of the stator circuit, with L_{ls} and L_{ms} being the leakage and magnetising inductance of the stator windings. Likewise, the elements of matrices $[RL_{r1}]$ and $[RL_{r2}]$ refer to rotor circuit one and two, respectively.

Thus,

$$[RL_{r1}] = \left[\begin{bmatrix} R_{aar1} & 0 & 0 \\ 0 & R_{bbr1} & 0 \\ 0 & 0 & R_{ccr1} \end{bmatrix} + \begin{bmatrix} L_{lr1} + L_{mr1} & -\frac{1}{2}L_{mr1} & -\frac{1}{2}L_{mr1} \\ -\frac{1}{2}L_{mr1} & L_{lr1} + L_{mr1} & -\frac{1}{2}L_{mr1} \\ -\frac{1}{2}L_{mr1} & -\frac{1}{2}L_{mr1} & L_{lr1} + L_{mr1} \end{bmatrix} \right] \quad (3.4.16)$$

and

$$[RL_{r2}] = \left[\begin{bmatrix} R_{aar2} & 0 & 0 \\ 0 & R_{bbr2} & 0 \\ 0 & 0 & R_{ccr2} \end{bmatrix} + \begin{bmatrix} L_{lr2} + L_{mr2} & -\frac{1}{2}L_{mr2} & -\frac{1}{2}L_{mr2} \\ -\frac{1}{2}L_{mr2} & L_{lr2} + L_{mr2} & -\frac{1}{2}L_{mr2} \\ -\frac{1}{2}L_{mr2} & -\frac{1}{2}L_{mr2} & L_{lr2} + L_{mr2} \end{bmatrix} \right] \quad (3.4.17)$$

Matrices $[L_{sr1}]$ and $[L_{sr2}]$ represent the mutual inductance between the stator and each rotor winding. Due to the physical location of the rotor windings with respect to the stator windings, both matrices are equal. The mutual inductance between the stator and the rotor windings $[L_{sr1}]$ is obtained from equation 2.3.9 which gives

$$[L_{sr1}] = L_{SR} \begin{bmatrix} \cos(\theta_r) & \cos\left(\theta + \frac{2\pi}{3}\right) & \cos\left(\theta - \frac{2\pi}{3}\right) \\ \cos\left(\theta - \frac{2\pi}{3}\right) & \cos(\theta_r) & \cos\left(\theta + \frac{2\pi}{3}\right) \\ \cos\left(\theta + \frac{2\pi}{3}\right) & \cos\left(\theta - \frac{2\pi}{3}\right) & \cos(\theta_r) \end{bmatrix} \quad (3.4.18)$$

in which the amplitude of the magnetising inductance is

$$L_{SR} = \frac{2}{3}KL_m \quad (3.4.19)$$

where L_m is the magnetising inductance referred to previously as Z_m , and K is the effective turns ratio.

The mutual inductance between the phases of rotor circuit one and rotor circuit two is obtained through the matrix $[L_{r1r2}]$. This inductance matrix describes the electromagnetic coupling between like phases and dissimilar phases in the rotor circuits and is given by

$$[L_{r1r2}] = \begin{bmatrix} L_{mr12} & -\frac{1}{2}L_{mr12} & -\frac{1}{2}L_{mr12} \\ -\frac{1}{2}L_{mr12} & L_{mr12} & -\frac{1}{2}L_{mr12} \\ -\frac{1}{2}L_{mr12} & -\frac{1}{2}L_{mr12} & L_{mr12} \end{bmatrix} \quad (3.4.20)$$

It is important to note that $[L_{r2r1}] = [L_{r1r2}]^T$.

At this point we have developed the complete voltage equations of the machine circuits with the constant and time varying mutual inductances. All the inductances will be discretized to form equivalent resistances and history voltage sources. A system of equations is formed from the resulting network of discretized inductances. In the next section the mathematical method will be formulated that solves the system of equation to obtain the stator and rotor currents.

3.5 Machine Circuit Model Formulation

The stator and rotor circuits phase voltage equations expressed in compact matrix form in expression 3.3.14 give a complete account of the interdependence of electrical and magnetic characteristics of the machine. The objective now is to discretize the differential equations and solve for the stator and rotor currents in the time domain. Phasor expression 3.3.14 in the time domain becomes

$$[V_s(t)] = p[[RL_s][I_s(t)] + p[[L_{sr1}(t)][I_{r1}(t)] + p[[L_{sr2}(t)][I_{r2}(t)] \quad (3.5.1)$$

$$[V_{r1}(t)] = p[[L_{r1s}(t)][I_s(t)] + p[[RL_{r1}][I_{r1}(t)] + p[[L_{r1r2}][I_{r2}(t)] \quad (3.5.2)$$

$$[V_{r2}(t)] = p[[L_{r2s}(t)][I_s(t)] + p[[L_{r2r1}][I_{r1}(t)] + p[[RL_{r2}][I_{r2}(t)] \quad (3.5.3)$$

The differential equations are solved, and in the case of the squirrel-cage induction motor the rotor phase voltages are made equal to zero. In this case the equations 3.5.1 - 3.5.3 changes to

$$[V_s(t)] = [RLE_s][I_s(t)] + [LE_{sr1}][I_{r1}(t)] + [LE_{sr2}][I_{r2}(t)] + [E_{sh}(t)] \quad (3.5.4)$$

$$[0] = [LE_{r1s}][I_s(t)] + [RLE_{r1}][I_{r1}(t)] + [LE_{r1r2}][I_{r2}(t)] + [E_{r1h}(t)] \quad (3.5.5)$$

$$[0] = [LE_{r2s}][I_s(t)] + [LE_{r2r1}][I_{r1}(t)] + [RLE_{r2}][I_{r2}(t)] + [E_{r2h}(t)] \quad (3.5.6)$$

Where $[RLE_s]$, $[RLE_{r1}]$, $[RLE_{r2}]$, $[LE_{sr1}]$, $[LE_{sr2}]$, $[LE_{r2s}]$, $[LE_{r1s}]$, $[LE_{r1r2}]$ and $[LE_{r2r1}]$ are matrices of equivalent resistances. The history voltage sources in each phase of the machine stator and rotor circuits are represented by the vectors $[E_{sh}(t)]$, $[E_{r1h}(t)]$ and $[E_{r2h}(t)]$. Where

$$[E_{sh}(t)] = [RLE_{sh}][I_s(t - \Delta t)] - [LE_{sr1h}][I_{r1}(t - \Delta t)] - [LE_{sr2h}][I_{r2h}(t - \Delta t)] - [V_s(t - \Delta t)] \quad (3.5.7)$$

$$[E_{r1h}(t)] = [RLE_{r1r1h}][I_{r1}(t - \Delta t)] - [LE_{r1sh}][I_s(t - \Delta t)] - [LE_{r1r2h}][I_{r2}(t - \Delta t)] \quad (3.5.8)$$

$$[E_{r2h}(t)] = [RLE_{r2r2h}][I_{r2}(t - \Delta t)] - [LE_{r2sh}][I_s(t - \Delta t)] - [LE_{r2r1h}][I_{r1}(t - \Delta t)] \quad (3.5.9)$$

In equations (3.5.7 - 3.5.9) the current vectors are the history current values in the respective phases. In these equations we can also establish that $[LE_{sr1h}] = [LE_{sr2h}] = [LE_{sr1}]$, $[LE_{r1r2h}] = [LE_{r1r2}]$ and that

$$[RLE_{sh}] = \left[\begin{bmatrix} R_{aas} & 0 & 0 \\ 0 & R_{bbs} & 0 \\ 0 & 0 & R_{ccs} \end{bmatrix} - \frac{2}{\Delta t} \begin{bmatrix} L_{ls} + L_{ms} & -\frac{1}{2}L_{ms} & -\frac{1}{2}L_{ms} \\ -\frac{1}{2}L_{ms} & L_{ls} + L_{ms} & -\frac{1}{2}L_{ms} \\ -\frac{1}{2}L_{ms} & -\frac{1}{2}L_{ms} & L_{ls} + L_{ms} \end{bmatrix} \right] \quad (3.5.10)$$

The structure of the equivalent resistance matrices $[RLE_{r1r1h}]$ and $[RLE_{r2r2h}]$ are similar to that shown for $[RLE_{sh}]$ in 3.5.10. The discretized circuit of the induction motor is shown in figure 18 (in an effort to avoid confusion in the drawing not all discretized inductances have been shown).

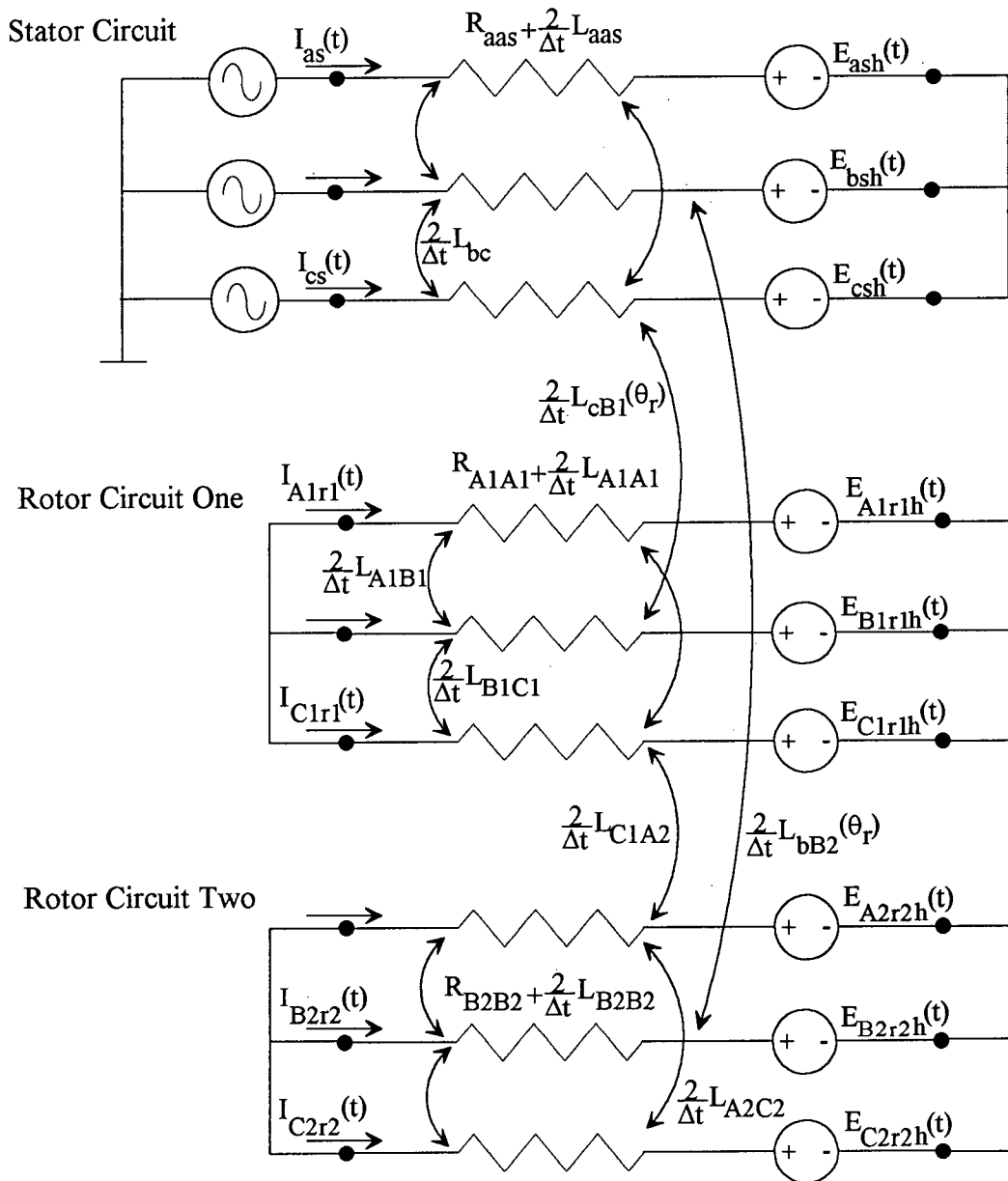


Fig. 18. Discrete-time model of the induction motor in phase coordinates.

By separating terms in expressions 3.5.6 and 3.5.5 we can obtain the vector of phase currents in both rotor circuits. The current vectors are

$$[I_{r2}(t)] = [RLE_{r2r2}]^{-1} \{-[E_{r2h}(t)] - [LE_{r2s}][I_s(t)] - [LE_{r2r1}][I_{r1}(t)]\} \quad (3.5.11)$$

$$[I_{r1}(t)] = \{[RLE_{r1}] - [LE_{r1r2}][RLE_{r2}]^{-1}[LE_{r2r1}]\}^{-1} \{ \{ [LE_{r1r2}][RLE_{r2}]^{-1} [LE_{r2s}] - [LE_{r1s}] \} [I_s(t)] - [E_{r1h}] + [LE_{r1r2}][RLE_{r2}]^{-1}[E_{r2h}] \} \quad (3.5.12)$$

Substituting the current vectors for both rotor circuits in 3.5.4 gives a single expression with all the electrical parameters of the machine. This expression establishes the link between the input voltage at the machine terminals and the parameters that determine its characteristics. Thus, after substitution and rearrangement of variables expression 3.5.4 becomes

$$\begin{aligned} [V_s(t)] = & \{ [RLE_s] + \{ [RLE_{r1}] - [LE_{r1r2}][RLE_{r2}]^{-1}[LE_{r2r1}] \}^{-1} \{ [LE_{sr1}] \\ & \{ [LE_{r1r2}][RLE_{r2}]^{-1}[LE_{r2s}] - [LE_{r1s}] \} \} - [LE_{sr2}][RLE_{r2}][LE_{r2s}] - \\ & \{ \{ [RLE_{r1}] - [LE_{r1r2}][RLE_{r2}]^{-1}[LE_{r2r1}] \}^{-1} \{ \{ [LE_{sr2}][RLE_{r2}]^{-1}[LE_{r2r} \\ & \{ [LE_{r1r2}][RLE_{r2}]^{-1}[LE_{r2s}] - [LE_{r1s}] \} \} \} \} [I_s(t)] \\ & \{ \{ [RLE_{r1}] - [LE_{r1r2}][RLE_{r2}]^{-1}[LE_{r2r1}] \}^{-1} \{ -[LE_{sr1}] + [LE_{sr2}][RLE_{r2}]^{-1} \\ & [LE_{r2r1}] \} \} [E_{r1h}(t)] + \{ (-[LE_{sr2}][RLE_{r2}]^{-1}) + \{ [RLE_{r1}] - [LE_{r1r2}][RLE_{r2}]^{-1} \\ & [LE_{r2r1}] \}^{-1} \{ [LE_{sr1}][LE_{r2r1}][RLE_{r2}]^{-1} - ([LE_{sr2}][RLE_{r2}]^{-1}[LE_{r2r1}][LE_{r1r2}] \\ & [RLE_{r2}] \} \} [E_{r2h}(t)] + [E_{sh}(t)] \end{aligned} \quad (3.5.13)$$

In this equation $V_s(t)$ is the vector of the machine terminal voltage supplied by the network to which it is connected.

Upon close observation of 3.5.13 one can divide the expression into two distinct parts; one portion is made up of an equivalent resistance matrix multiplied by the current vector $I_s(t)$, while the other is an equivalent history source. Thus, expression 3.5.13 can be reduced to

$$[V_s(t)] = [RLeq_s][I_s(t)] + [Eeq_h(t)] \quad (3.5.14)$$

where $[RLeq_s]$ is the equivalent resistance matrix of a three phase network and $[Eeq_h]$ is a vector representing the history voltages in the three phases of the network. Therefore, the induction machine with its stator and two rotor circuits has been reduced to a simple three phase network of equivalent resistances with a voltage source in each phase. It is important to emphasise that all the physical phenomena that occurs when the machine is in motion are preserved in this new circuit representation. From the expression 3.5.14 the stator phase currents of the machine can be determined when it is energised by a source whose phase voltage is $V_s(t)$.

Chapter Four

Electromechanical Equations And Data Requirements For The New Model

The transformation from electrical energy to mechanical energy in the induction motor occurs across the machine air gap. This transfer of energy across the machine air gap is made possible by the magnetic coupling that exists between the stator and rotor circuits. Therefore, the magnetic field acts as the agent for the transportation of the energy. In this chapter we will look at the mechanism for the development of energy in the machine air-gap magnetic field and its importance in the complete energy conversion process from electrical to mechanical energy.

In chapter three we looked at the development of the electrical circuit model of the machine and it was observed that some of the data required by the PDTM are not normally supplied by the manufacturers of induction machines. Therefore, in this chapter we will briefly describe the modifications made to a computer program developed by Ricky Hung and H. W. Dommel [16] to obtain the necessary circuit parameters to perform transient simulations with the PDTM.

4.1 Torque Production in the Induction Machine

Generally, induction machines are considered highly efficient electrical apparatus. Most of the electrical energy supplied from the network is transformed to mechanical energy, with the remainder as losses due to winding resistance, friction and windage, and field losses. In utilising the energy concept to obtain an expression for the electromagnetic

torque in the motor it is assumed that the magnetic circuit is linear which implies that there can be no losses in the magnetic field.

The production of electromagnetic torque in the induction motor is inextricably linked to the energy in the machine magnetic field. Therefore, we now look at the energy in the machine magnetic field. This energy is that which is contained in the self and mutual inductances of the stator, the magnetising inductance between stator and rotor, and the rotor self and mutual inductances. The energy in the machine coupling field (W_p) at every instant in time during the machine transient or steady-state operation can be determined by

$$\begin{aligned}
 W_p(t) = & \frac{1}{2} [I_s(t)]^T \{ [L_s] - [Ll_s] \} [I_s(t)] + [I_s(t)]^T [L_{sr1}(t)] [I_{r1}(t)] + \\
 & [I_s(t)]^T [L_{sr2}(t)] [I_{r2}(t)] + \frac{1}{2} [I_{r1}(t)]^T \{ [L_{r1}]' - [Ll_{r1}]' \} [I_{r1}(t)] + \\
 & \frac{1}{2} [I_{r2}(t)]^T \{ [L_{r2}]' - [Ll_{r2}]' \} [I_{r2}(t)] \quad (4.1.1)
 \end{aligned}$$

where;

$[L_s]$ is the matrix of the stator self and mutual inductance,

$[Ll_s]$ is the diagonal matrix of the stator leakage inductance,

$[Ll_{r1}]'$ is the diagonal matrix of the rotor circuit one referred to the stator,

$[Ll_{r2}]'$ is the diagonal matrix of the rotor circuit two referred to the stator,

$[L_{r1}]'$ is the matrix of the rotor circuit one self and mutual inductance,

$[L_{r2}]'$ is the matrix of the rotor circuit two self and mutual inductance,

$[I_s(t)]$ is the vector of the stator phase currents,

$[I_{r1}(t)]'$ and $[I_{r2}(t)]'$ are the vectors of the rotor circuits phase currents referred to the stator,

$[L_{sr1}(t)]'$ and $[L_{sr2}(t)]'$ are the matrices representing the mutual inductance between the stator and the rotor circuit one and two respectively.

The linkage between the energy in the coupling field and the change of mechanical energy in the rotating machine is expressed as

$$dW_m = -T_e \left(\frac{2}{p} \right) d\theta_r \quad (4.1.2)$$

where dW_m is the change in mechanical energy of the machine rotor, T_e is the electromagnetic torque, p the number of poles in the machine and θ_r is the electrical angular displacement of the rotor.

The machine electromagnetic torque is proportional to the change of energy in the coupling field. However, the energy in the coupling field of the machine depends on the current in the circuits and the angular position of the rotor. The latter determines the value of the mutual inductance between the stator and rotor circuits. Therefore, we may express the electromagnetic torque as

$$T_e(i_j, \theta_r) = \frac{p}{2} \frac{dW_f(i_j, \theta_r)}{d\theta_r} \quad (4.1.3)$$

which expands to give

$$T_e(\theta_r) = \frac{p}{2} [I_s(t)]^T \frac{d}{d\theta_r} [L'_{sr1}(\theta_r)] [I_{r1}(t)]' + \frac{p}{2} [I_s(t)]^T \frac{d}{d\theta_r} [L'_{sr2}(\theta_r)] [I_{r2}(t)] \quad (4.1.4)$$

In our transient analysis of the electromagnetic torque the change in the electrical angular position of the rotor occurs during the time step " Δt ", therefore, we can consider the torque in each time step. In effect one should consider that the mutual inductance between stator and rotor changes with time. Thus, equation 4.1.4 becomes

$$T_e(t) = \frac{p}{2} [I_s(t)]^T \frac{d}{d\theta} [L'_{sr1}(t)] [I_{r1}(t)]' + \frac{p}{2} [I_s(t)]^T \frac{d}{d\theta_r} [L'_{sr2}(t)] [I_{r2}(t)] \quad (4.1.5)$$

The electrical and the mechanical properties of an induction motor are combined in equation 4.1.6. This equation relates the electromagnetic torque developed in the machine with the moment of inertia and speed of the rotor. Thus, this electromagnetic torque is

$$T_e(t) = J_e \frac{d\omega_r(t)}{dt} + \frac{2}{p} T_L \quad (4.1.6)$$

where J_e is the moment of the rotor, T_L is the load torque and $\omega_r(t)$ is the electrical angular velocity of the rotor. The discretization of this differential equation using the trapezoidal rule of integration gives

$$\omega_r(t) = \omega_r(t - \Delta t) + \frac{\Delta t}{J_e} \{T_e(t) + T_e(t - \Delta t)\} - \frac{2\Delta t}{pJ_e} \{T_L(t) + T_L(t - \Delta t)\} \quad (4.1.7)$$

This equation is used to determine the velocity of the rotor at each time step during a transient simulation study.

4.2 Predicting Rotor Velocity and Angular Position

When the PDTM is used in simulation studies the rotor position and velocity must be predicted at each time step. The rotor speed is predicted based on linear extrapolation. In this method the previous two history values are used to determine the speed at the time step being simulated. The error that occurs in a prediction scheme of this nature is very small, especially in situations where the time step is in the order of microseconds. This is due to the difference between the large time constant of the rotating masses compared with that of the electrical circuit. Therefore, the predicted rotor speed is given by

$$\omega(t) = 2\omega(t - \Delta t) - \omega(t - 2\Delta t) \quad (4.2.1)$$

The angular position and rotor velocity are related by $\omega = \frac{d\theta}{dt}$, which, after discretization with the trapezoidal rule of integration gives

$$\theta(t) = \theta(t - \Delta t) + \frac{\Delta t}{2} \omega(t) + \omega(t - \Delta t) \quad (4.2.2)$$

Here $\theta(t)$ is the rotor position as determined by the predicted speed $\omega(t)$ in equation (4.2.1). $\omega(t - \Delta t)$ is the speed of the rotor at the previous time step.

4.3 Data for the PDTM Program

Besides the standard data supplied by the manufacturers of squirrel cage induction machines, the phase domain transient model developed in this thesis requires that additional machine parameters be known. On rare occasions some manufacturers would provide machine users with a substantial amount of data relating to the equivalent circuit. However, it is widely acknowledged that these parameters are not sufficiently reliable to be used in performing transient studies [9]. Consequently, a program capable of calculating with greater precision the electrical parameters of the equivalent circuit of figure 5 was developed [16] to be used with the induction motor model in the EMTP. This program requires the input of basic motor starting and steady-state performance characteristics such as: rated voltage and efficiency, power factor at rated load, rated load, starting torque and maximum torque, starting current at rated voltage as well as starting current at reduced starting voltage. The program uses this information as a package to obtain the following parameters of the 60-Hz equivalent circuit: stator and rotor resistances, stator leakage reactance, rotor leakage reactance, stator-rotor magnetising reactance, and the mutual reactance between rotor circuits. However, the data required to perform transient simulations with the PDTM are: stator and rotor resistances, stator leakage inductance, stator circuit mutual inductance, rotor leakage inductance, mutual inductance between phases of the rotor circuits, and the mutual inductance between the two rotor circuits. The close similarity between the circuit parameters of the 60-Hz equivalent circuit and the circuit parameters required by the PDTM makes it possible to use the former as a base to obtain the requirements of the latter.

The first procedure in the modifications done to the program was to convert all per unit quantities to physical units. These quantities in the form of resistances and inductances are then used in conjunction with the procedure described in section 3.4 to obtain all the parameters necessary to perform transient simulations with the PDTM. In this analysis it is important to consider the relationship between the amplitude of the stator-rotor mutual inductance [L_{SR}] and the stator mutual inductance [L_{ms}] with the stator-rotor magnetising inductance [L_m]. These are expressed as follows

$$L_{SR} = \frac{2}{3}KL_m \quad (4.3.1)$$

$$L_{ms} = \frac{2}{3}L_m \quad (4.3.2)$$

The modifications made to the program developed in [16] makes it possible to obtain all the parameters needed by the PDTM by providing the same input data provided by the motor manufacturer as would be required for a transient simulation with the EMTP.

Chapter Five

Transient Simulation With The Phase-Domain Transient Model

In this chapter we will test the new model by performing three scenarios of startup transient simulations. The "cold" motor startups will be carried out with no mechanical load on the machine shaft, a constant mechanical load, and finally a third load that varies with the speed. The simulations that will be presented are just a few in a number of different types of studies that can be performed with the new phase-domain transient model. Transient simulations will be performed on a large motor pump with a nominal output of 11,000 Hp. The results from the PDTM program for the 11,000 Hp pump motor will be compared with those from the EMTP for the same motor. This comparison is used to assess the validity of the proposed phase-domain method of modelling the induction motor.

5.1 Simulation Studies

This section presents the results from the simulation of an 11,000 Hp pump motor. This is a large induction motor that can found in nuclear generating stations, pulp and paper manufacturing plants, and large oil and gas pumping stations in remote locations. Because of the size of this motor, and consequently its high starting current and large moment of inertia, it is important to know its starting characteristics under different load conditions. These starting characteristics include the starting time, the magnitude and form of the starting current, as well as the torque characteristics for a given supply, and

the speed of the rotor when it reaches steady-state conditions. These characteristics represent of the induction motor will be analysed in the simulations with this machine.

The data of the motor as supplied by the manufacturer is as follows [8]:

rated power = 11,000 Hp,

rated voltage = 6.6 kV,

efficiency = 98.5 %,

power factor = 0.906,

starting torque at rated voltage = 1.47 p.u.,

maximun torque = 3.5 p.u.,

rated slip = 0.00622,

starting current at rated voltage = 8.0 p.u.,

reduced starting voltage = 0.785 p.u., and

starting current at reduced starting voltage = 6.03 p.u.

These data were supplied to the circuit parameter calculation program discussed in section 4.4. This program calculates the circuit parameters for the standard 60-Hz double-cage equivalent circuit and those required by the phase-domain transient model program. The circuit parameters used in the PDTM program to perform the simulations with this motor are as follows:

stator resistance = 0.02172 ohm,

resistance of rotor circuit one = 0.11869 ohm,

resistance of rotor circuit two = 0.04136 ohm,

stator leakage inductance = 0.00080 H,

stator magnetising inductance = 0.02591 H,

amplitude of the mutual inductance between stator and rotor = 0.02591 H,

leakage inductance of rotor circuit two = 0.00146 H,

mutual inductance of rotor circuits = 0.000701 H,

For the startup simulation a reactor of 0.2 ohm is connected in series with the motor to limit the initial current. The following simulations were performed:

(a) Motor startup with no load on the rotor shaft.

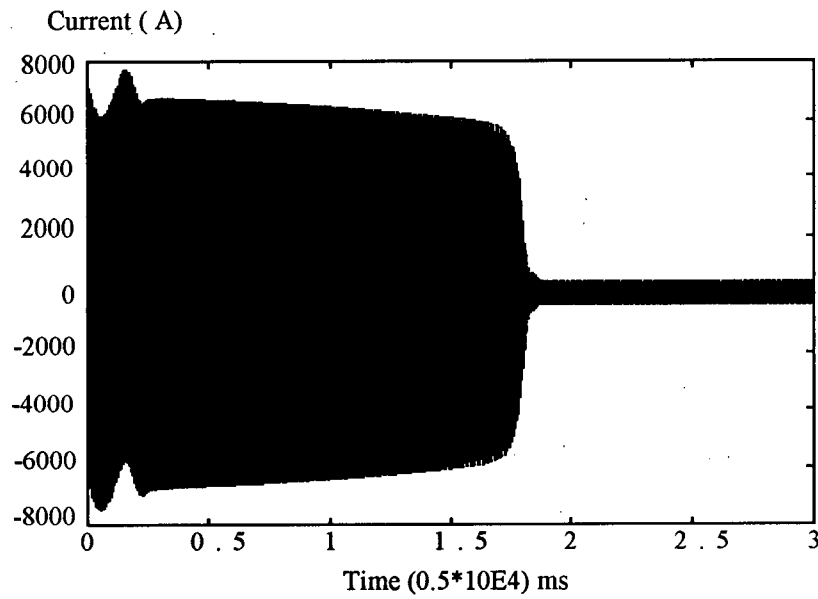


Fig. 19. No-load stator current (phase a) during startup.

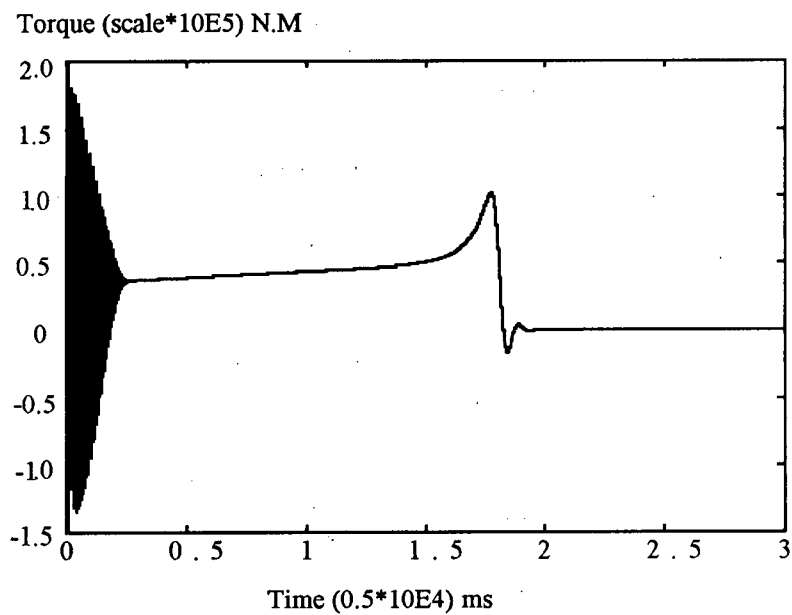


Fig. 20. Torque characteristics during no-load startup.

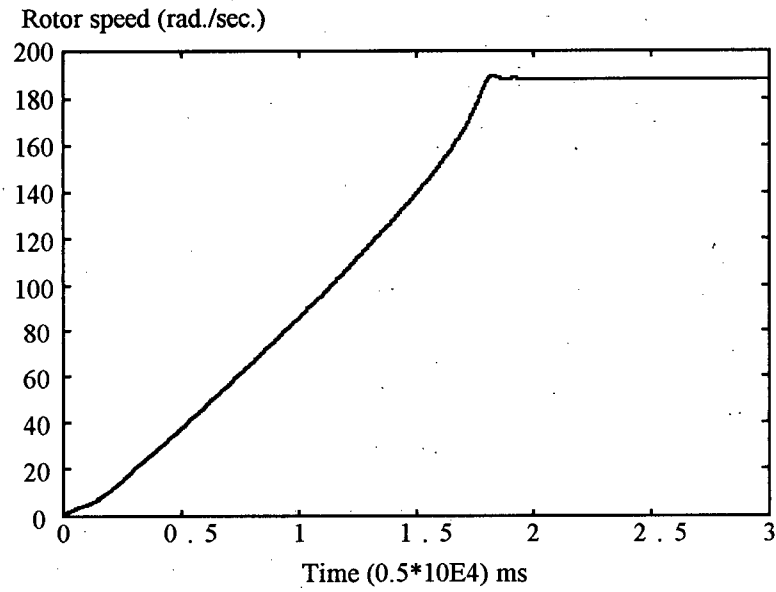


Fig. 21. Rotor speed during no-load startup.

(b) Motor startup with a mechanical load that varies with its rotor speed

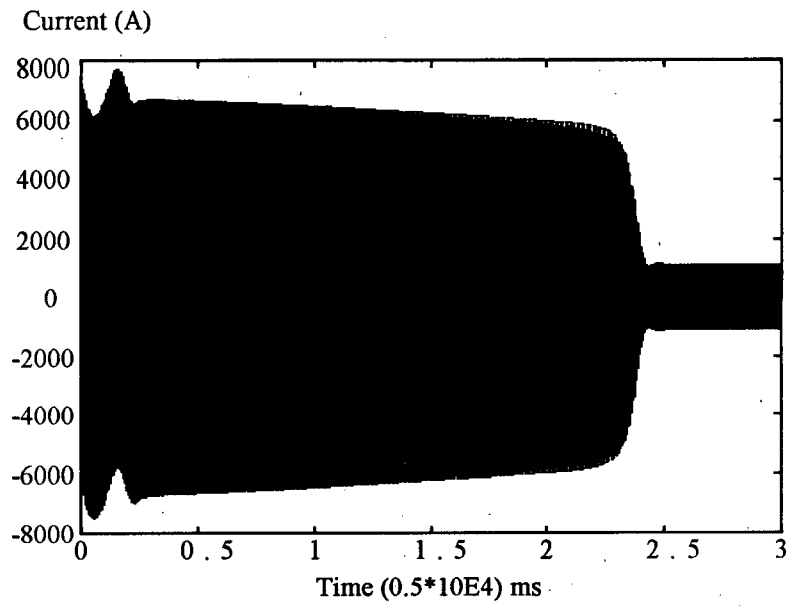


Fig. 22. Startup stator current (phase a) with a transient mechanical load.

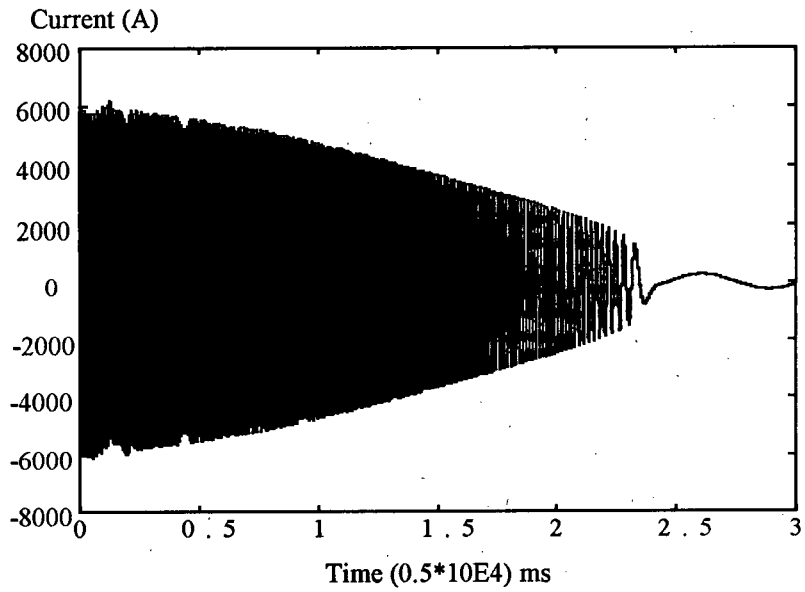


Fig.23. Outer rotor startup current (phase a) with a transient mechanical load.

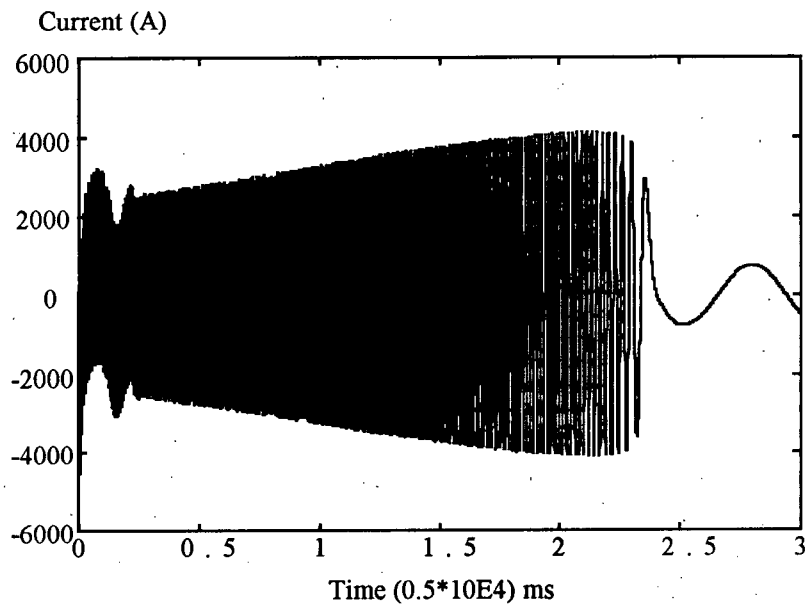


Fig. 24. Inner rotor startup current (phase a) with a transient mechanical load.

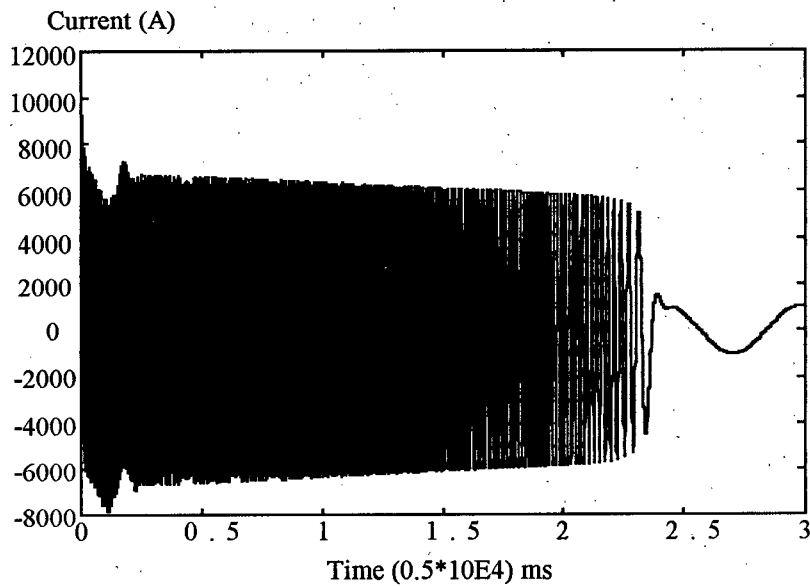


Fig. 25. Total startup rotor current with a transient mechanical load.

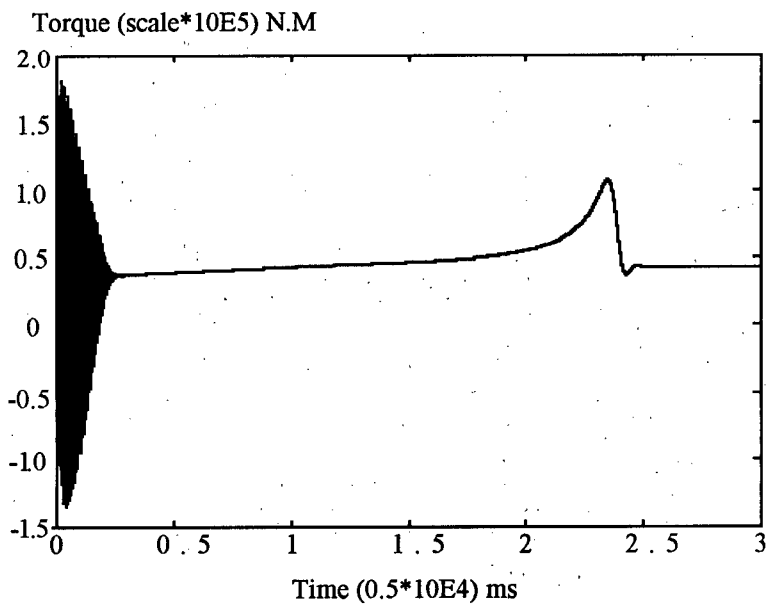


Fig. 26. Motor torque Characteristics during startup with a transient mechanical load.

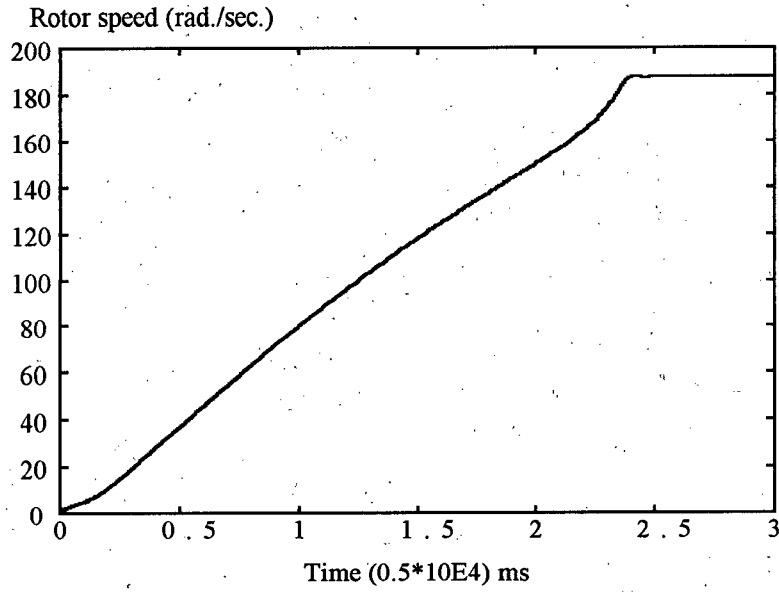


Fig. 27. Rotor speed during motor startup with transient a mechanical load.

(c) Motor startup with a constant mechanical load

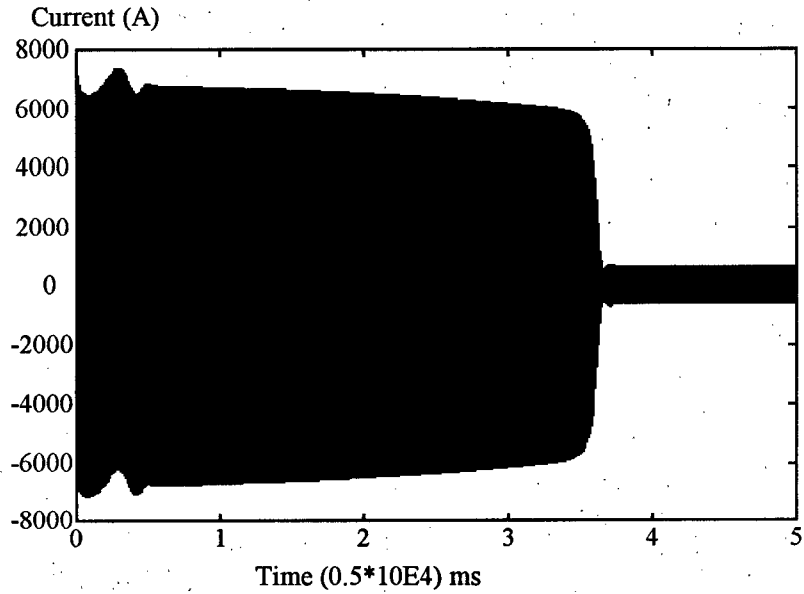


Fig. 28. Stator current (phase a) during startup with constant mechanical load.

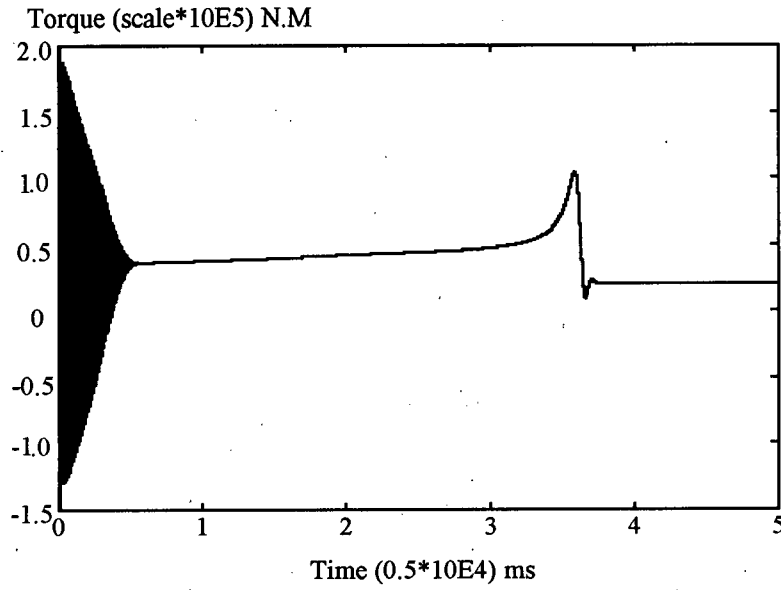


Fig. 29. Torque characteristics during startup with constant mechanical load.

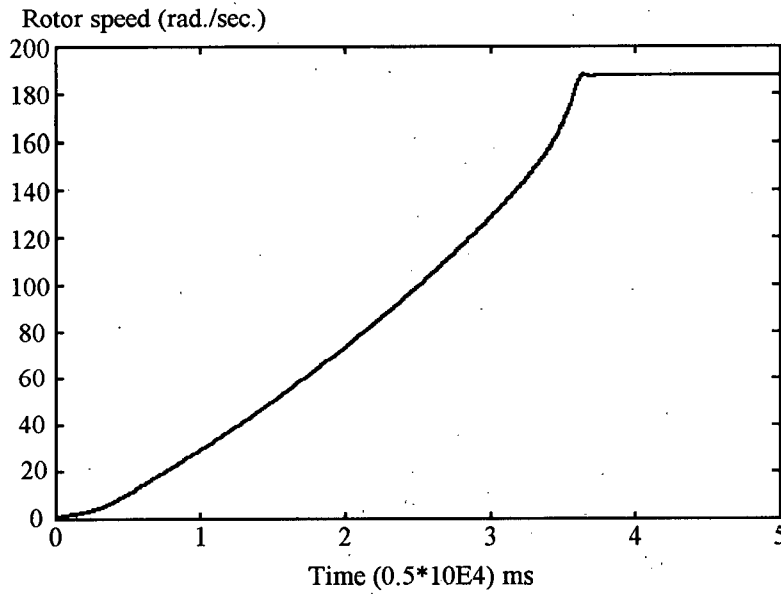


Fig. 30. Rotor speed during startup with constant mechanical load.

The EMTP is widely recognised as the standard tool for electromagnetic transient simulations in the field of power engineering. This program uses the conventional dq0 coordinate transformation to represent the machine variables. To compare the results from the phase-domain model with those from the EMTP, the 11,000 Hp motor was simulated using both methods. The simulations were performed in both cases with a supply phase voltage of 5550 volts and a starting reactor of 0.2 ohm in each phase. These simulations were done with a mechanical load that varied with the speed of the rotor. The results are shown in figures 31 to 36.

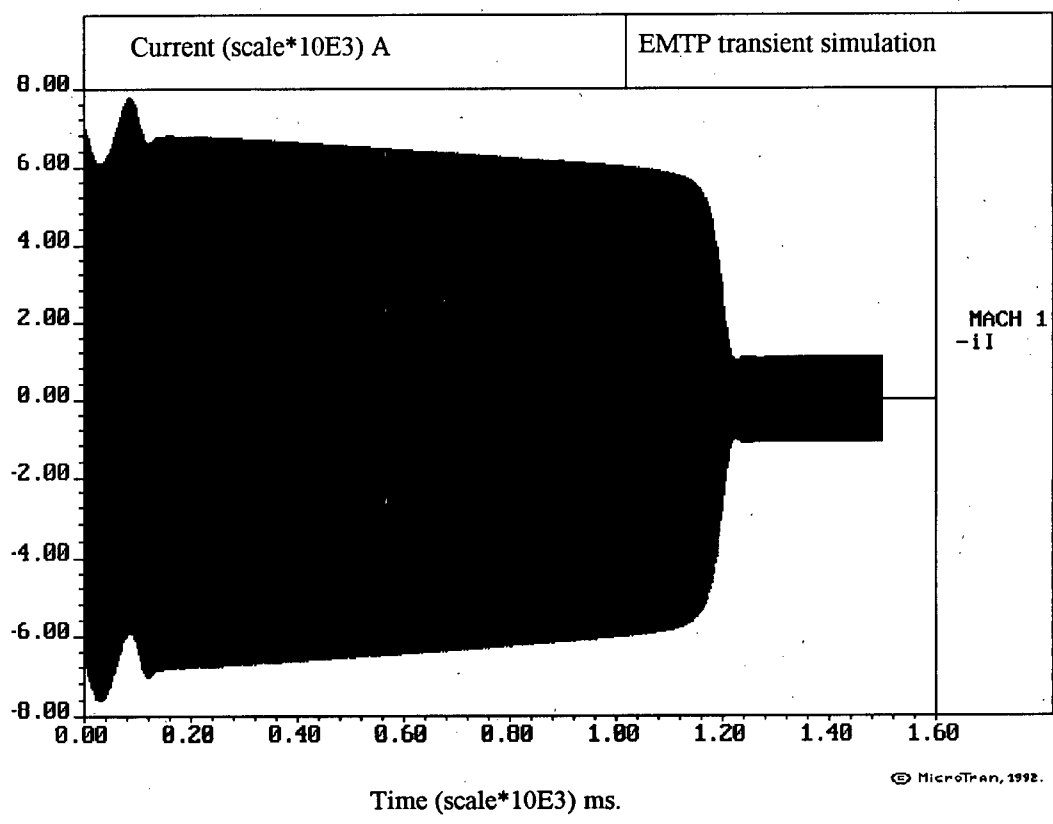


Fig. 31. EMTP simulated stator current (phase a).

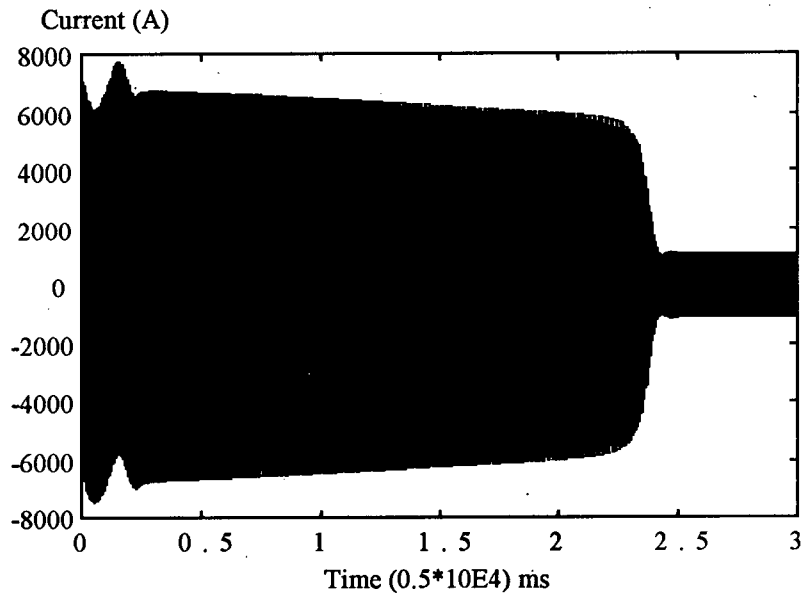


Fig. 32. Stator current (phase a) simulated with the phase-domain transient model.

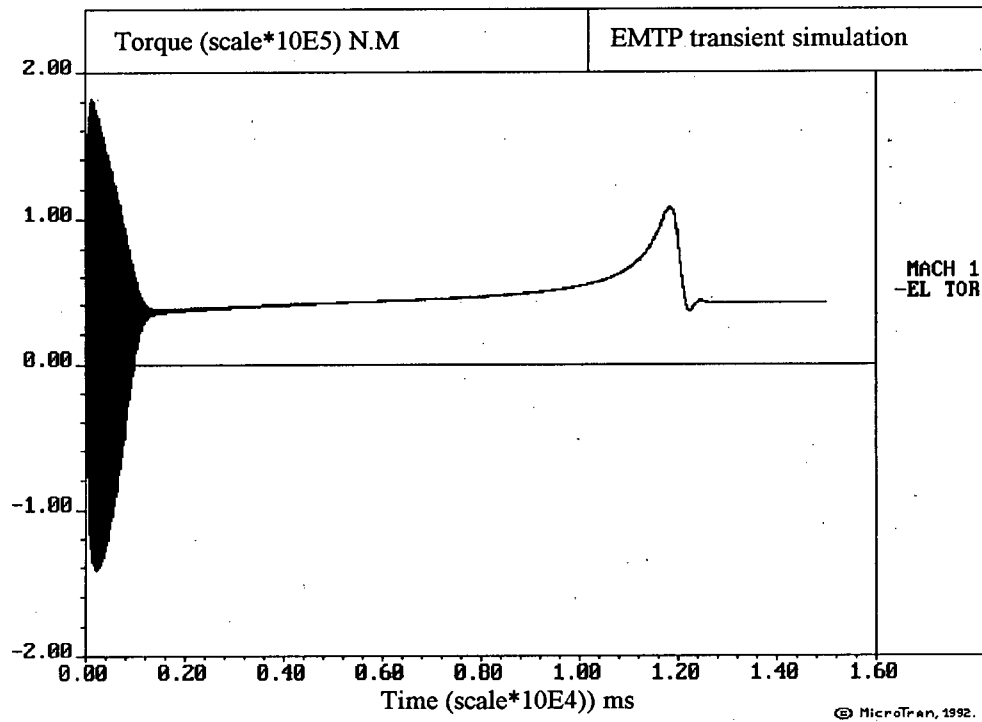


Fig. 33. Motor Torque characteristics simulated with the EMTP.

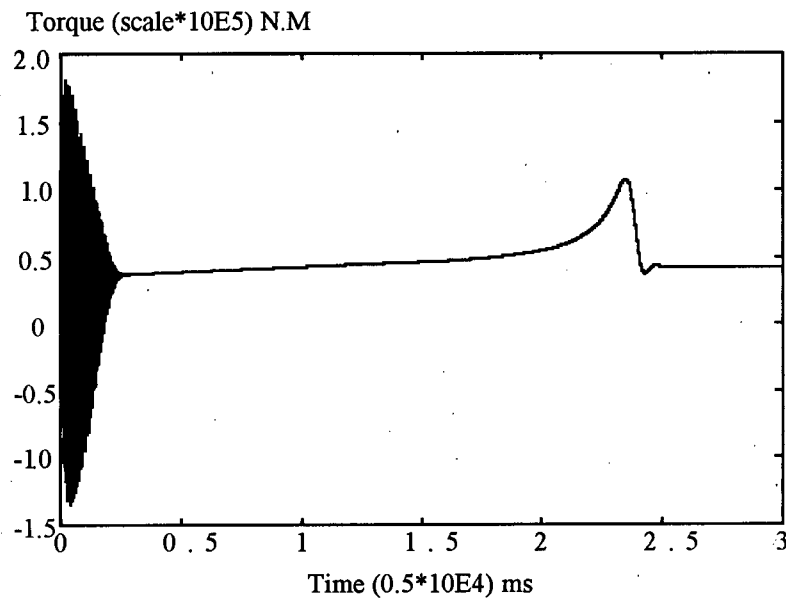


Fig. 34. Motor torque characteristics simulated with the phase-domain transient model.

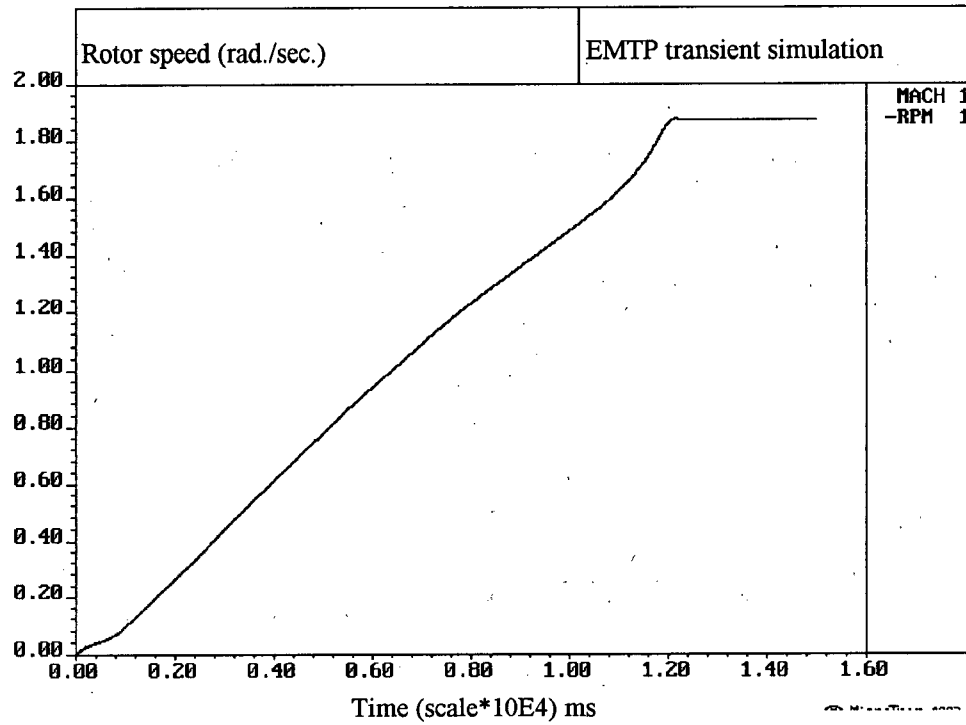


Fig. 35. Rotor speed simulated with the EMTP.

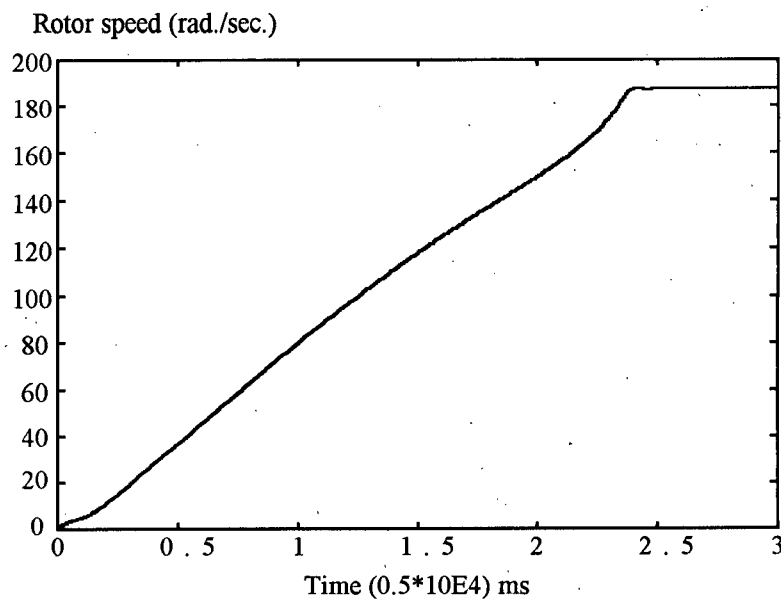


Fig. 36. Rotor speed simulated with the phase-domain transient model.

From the results presented in the preceding figures it can be seen that the results from the phase phase-domain transient model program matches closely those obtained with the EMTP. These results demonstrate that the phase-domain transient model program can be used to perform transient simulations that have previously been done with the EMTP.

Conclusions

In power utilities all system variables are given values in the phase-coordinate system. At the same time, standard measuring techniques simulate parameters such as voltages, currents, and impedances in phase quantities. Therefore, it would be convenient and more accurate in many cases if power system engineers were to possess the tools capable of performing transient and steady-state simulation of these systems or components of the system in the phase-domain. In this thesis, a philosophy and methodology have been presented which offers this possibility. The phase-domain transient model of the induction motor performs transient and steady-state analyses with the machine circuit parameters and variables directly in the phase-domain.

The accuracy of the PDTM program for the induction machine compares favourably with that of the most established electromagnetic transient program (EMTP). This is confirmed by the transient simulation results presented in chapter five. The algorithm used in the phase-domain model is quite simple. The implementation is made easier by the utilisation of the high-level and extremely flexible ADA 9X programming language to code the model. The object code is quite simple and offers the possibility of future development and extension to the model. The transient induction motor program has been developed for use on personal computers and simplicity in the area of human-machine interface was given top priority in its development.

The phase-domain transient model of the induction machine utilises a linear magnetic circuit. It is hoped that future work in this area would attempt to consider the nonlinearities in the magnetic circuit of the induction motor. This would improve the accuracy and flexibility of the model.

Induction machines of different types are extensively used in many commercial and industrial applications. However, this model in its present stage of development is only suitable for transient analysis of the squirrel-cage induction motor. It is hoped that future work in this area would concentrate on the development of a general model suitable for all types of induction machines (e.g. wound rotor motors and induction generators).

This transient model program of the induction squirrel-cage motor has immediate industrial application. However, it is anticipated that if this program is used in the teaching of induction motors it can present students with a clearer understanding of the principles and operation these machines.

Finally, it is hoped that with the presentation of this thesis a new and powerful tool has been initiated to further the development of online power system monitoring and supervision.

Bibliography

1. M. P. Kostenko and L. M. Piotrovsky, "Electrical Machines - part 2," foreign language publishing house, Mocsow.
2. Paul C. Krause, "Analysis of Electric Machinery," Mc Graw-Hill series in electrical engineering, power and energy (1986).
3. Prabha Kundur, "Power System Stability and control," Mc Graw-Hill Inc. - 1993.
4. George McPherson, "An Introduction to Electrical Machines and Transformers," John Wiley and Sons, Inc., 1981.
5. G. R. Slemon and A. Straughen, "Electric Machines," Addison-Wesley Publishing Company, Inc., 1982.
6. A. I. Voldek, "Electrical Machines - part 2", printed in the USSR - 1983.
7. G. J. Rogers, J. DiManno and R. T. Allen, "An Aggregate Induction Machine for Industrial Plants," IEEE Trans. PAS - 103, April 1984, pp. 683-690.
8. G. J. Rogers, and D. Shirmohammadi, "Induction Machine Modelling fot Electromagnetic Transient Program," IEEE Trans. on Energy conversion, Vol. EC - 2, No. 4, December 1987.
9. Samuel S. Walters, Ronald D. Willoughby, "Modelling Induction Motors for System Studies," IEEE Transactions on Industrial Applications, Vol. IA - 19, No. 5, September/October 1983, pp. 875 - 878.
10. Herman W. Dommel, "EMTP Theory Book," Second Edition, Microtran Power System Analysis Corporation, Vancouver, British Columbia, May 1992.
11. B. J. Chalmers and A. S. Mulki, "Design Synthesis of Double-Cage Induction Motors," Proc. IEE, Vol. 117, No. 7, July 1970, pp. 1257 - 1263.

12. Paul C. Krause and C. H. Thomas, "Simulation of Symmetrical Induction Machinery," IEEE Transactions PAS, Vol. PAS - 84, No. 11, November 1965.
13. Eugene A. Klingshirn and Howard E. Jordan, "Simulation of Polyphase Induction Machines With Deep Rotor Bars," IEEE Transactions PAS, Vol. PAS - 89, No. 6, July/August 1970.
14. Graham J. Rogers, "Demistifying Induction Motor Behaviour," IEEE Computer Applications in Power, January 1994.
15. Thomas A. Lipo and Alfio Consoli, "Modelling and Simulation of Induction Motors with Saturable Leakage Reactances," IEEE Transactions on Industry Applications, Vol. IA-20, No. 1, January/February 1984.
16. R. Hung and H. W. Dommel, "Synchronous Machine Models for Simulation of Induction Motor Transients", submitted to IEEE Power Engineering Society for IEEE Summer Power Meeting 1995.